Air Leakage of Insulated Concrete Form Houses

by

Hannah Durschlag
Bachelor of Science in Civil Engineering, 2010
Northwestern University
Evanston, IL

Submitted to the Department of Architecture
in partial fulfillment of the requirements for the degree of
Master of Science in Building Technology

at the
Massachusetts Institute of Technology

June 2012

Signature of Author……………………………………………………………………………………………...
Department of Architecture
May 11, 2012

Certified by……
John Ochsendorf
Associate Professor of Architecture and Civil and Environmental Engineering
Thesis Co-Supervisor

Certified by……
Leslie Keith Norford
Professor of Building Technology
Thesis Co-Supervisor

Accepted by………………………………………………………………………………………………………...
Takehiko Nagakura
Chair of the Department Committee on Graduate Students

Thesis Co-Advisor: John Ochsendorf, PhD
Associate Professor of Architecture and Civil and Environmental Engineering

Thesis Co-Advisor: Leslie Keith Norford, PhD
Professor of Building Technology

Air Leakage of Insulated Concrete Form Houses
by
Hannah Durschlag

Submitted to the Department of Architecture
On May 11, 2012 in partial fulfillment of the requirements
for the degree of Master of Science in Building Technology

Abstract
Air leakage has been shown to increase building energy use due to additional heating and cooling loads. Although many construction types have been examined for leakage, an exploration of a large number of Insulated Concrete Form (ICF) houses has not yet been completed. This thesis first collects 43 blower door tests of recently built ICF houses in North America. These are then examined and compared with a large collection of blower door tests of wood-stud construction. There is a 1.2% difference between ICF and wood-stud air leakage, with a very similar range. This range is mainly attributed to leakage from the attic space and cracks around windows based on a thorough investigation of two specific ICF houses in Nashville, TN. Using an EnergyPlus building model, the difference in air leakage between a typical ICF and wood-stud house in Chicago and Phoenix is not found to cause a significant gap in energy use. However, the range in air leakage does affect the amount of energy a single-family house consumes.

Thesis supervisor: John Ochsendorf
Title: Associate Professor of Architecture and Civil and Environmental Engineering

Acknowledgements
First, I would like to acknowledge Professors Ochsendorf and Norford. Thank you for the support and advice. You made it possible for me to come to MIT as a civil engineer and leave as a building scientist.

I would also like to recognize the Building Technology Lab. The people I have met here are both colleagues and friends. I greatly admire all the work that you do. In particular, thank you to Amanda Webb for contributing her expertise for Chapter 5 of this thesis.

This thesis would not have been possible without funding. Thank you to the Concrete Sustainability Hub and the Building Technology Department for supporting this work.

I would like to thank my friends, particularly the Northwestern Eight, for being there for me and always being able to make me laugh. I am so glad you are in my life.

Finally, a big thank you to my parents. I appreciate your constant love and support more than I can say.

Table of Contents

1. Introduction 6
1.1 Understanding building energy use 6
1.2 Air leakage 6
1.3 Insulated Concrete Form (ICF) 7
1.4 Structure of thesis 7
1.5 Summary 8
2. Literature Review 9
2.1 Introduction 9
2.2 Basics of air leakage 9
2.3 Infiltration of concrete structures 11
2.4 Air leakage variability 13
2.5 How infiltration affects energy use 14
2.6 Conclusions 16
3. The Air Leakage of Insulated Concrete Form Houses 17
3.1 Introduction 17
3.2 Experimental results from blower door testing 17
3.3 Leakage distribution 19
3.4 Leakage prediction 24
3.5 ICF compared to US houses 27
3.6 Conclusions 31
4. The Variability in the Air Leakage of Insulated Concrete Form Houses 32
4.1 Introduction 32
4.2 Thermal Imaging 33
4.3 Sequential Blower door testing 41
4.4. Consolidated Findings and Verification 45
4.5. Recommendations 47
4.6. Conclusions 48
5. Energy Use of Single Family Houses 49
5.1 Introduction 49
5.2 Creating the model 49
5.3 Infiltration in the model 52
5.4 The results 54
5.5 Discussion 56
5.6 Conclusions 57
6. Conclusions 58
Appendix A : Code Used for Analysis in Section 3.2 65
Appendix B : Chart Used to Collect Blower Door Data 66
Appendix C : Leakage Area, Floor Area and Height of the 31 Houses in the Dataset 68
Appendix D : ASTM Uncertainty Calculation 69
Appendix E : Code Used for Analysis in Section 3.3 70
Appendix F : Details of leakage prediction and code used for this analysis 72
Appendix G : Code Used for Analysis in Section 3.5 78

1. Introduction

1.1 Understanding building energy use

According to the Environmental Protection Agency, buildings consumed 39% of the total energy used in the United States in 2003 (EPA, 2009). The chart in Figure 1.1 displays the residential, commercial, and total energy use since 1990. A large portion of total energy use in the US is due to buildings. Energy use is increasing with time, but the percentage of building usage remains fairly consistent.

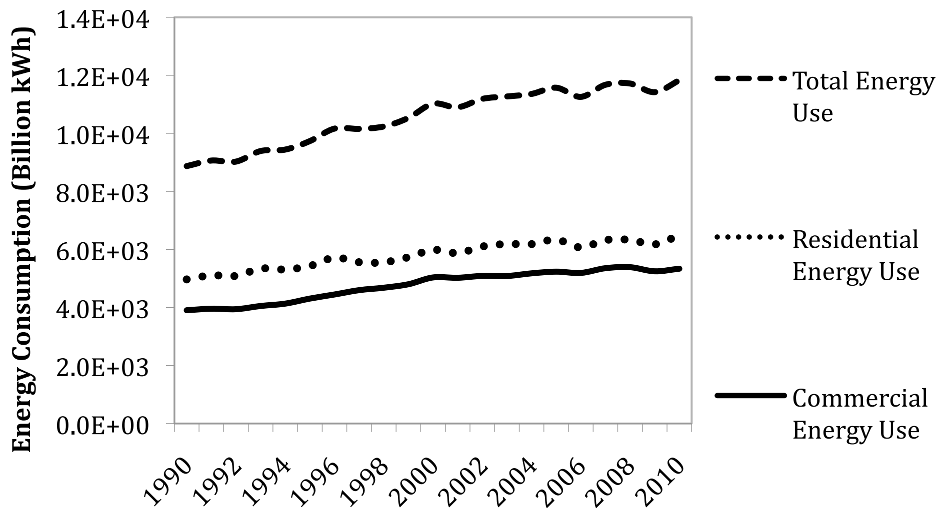

Figure 1.1 Total and building energy consumption in the United States illustrates the increase in energy use over time for all sectors (EPA, 2009).

In addition, approximately 44% of building energy in 2003 was used for heating and cooling (EPA, 2003). According to Balaras et al. (1999), the structure of a building and its corresponding design affect energy loss and consumption. Therefore, by understanding how design decisions influence heating and cooling loads, buildings can be modified to reduce energy consumption.

1.2 Air leakage

There are many aspects of building structure that can affect energy use. This thesis will focus on air leakage. A typical definition of air leakage is the movement of air into and out of unplanned openings in a building enclosure or envelope (Sherman and Chan, 2004). Examples of unplanned openings include cracks around windows or joints between the wall and the roof. A test used to measure the size of these holes is called a blower door test. This test determines the volume flow rate through cracks, the infiltration, and their total area, the leakage area. The blower door test will be explained in detail in Chapter 2.

Air leakage is the focus of this thesis due to its importance in energy loss and consumption. As will be examined in much more detail in the literature review in Chapter 2, between 16 and 33% of building energy consumption has been attributed to infiltration (Shaw and Jones, 1979) (Emmerich and Persily, 1998) (Sherman, 1985). In other studies, infiltration is responsible for between 7 and 46% of energy loss (Tamura and Shaw, 1977) (Balaras et al., 1999). These ranges are large and are associated with different types of structures and climates. Therefore, more precise numbers for specific building envelopes would be useful for making design decisions.

1.3 Insulated Concrete Form (ICF)

Due to the large percentage of building energy used by the residential sector, this thesis will focus on single-family housing. There are many different construction methods for single-family housing. Wood-stud construction is the most typical. Houses can also be built from cast-in-place concrete, pre-cast concrete, structural insulated panels, Insulated Concrete Form (ICF), and other options. This thesis will examine ICF single-family construction. The basic structure of ICF is two layers of two and one half inches polystyrene insulation, which are held together with metal or plastic ties. Concrete, generally six inches thick, is then poured between these two layers. The insulation acts as permanent formwork for the concrete and is not removed (Insulated Concrete Form Association, 1995). A representation of this geometry can be seen in Figure 1.2.

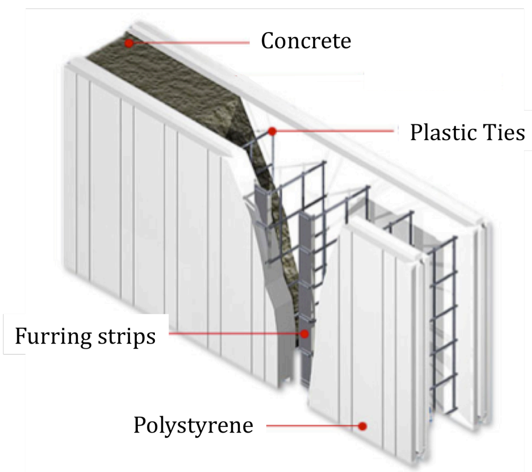

Figure 1.2. A schematic (left) and picture (right) of the Insulated Concrete Form which displays two layers of insulation, tied together. These act as permanent formwork for a layer of concrete (Rajagopalan et al., 2009) (http://www.concrete-home.com, 2006).

This thesis investigates ICF construction for several reasons. First, as will be shown in the literature review in Chapter 2, the air leakage of insulated concrete form houses has not yet been examined in detail. Next, because of the inherent continuity of the walls in ICF construction, there have been numerous claims of its potential for energy savings due to lower air leakage (ICF Facts, 2012) (ARXX ICF, 2012). There is clearly a hole in our knowledge of this building type that is necessary to address.

1.4 Structure of thesis

As described above, neither the air leakage of ICF houses nor their energy use has been examined in detail. This thesis examines three key questions:

1. What are the trends in air leakage of ICF single-family houses and how do they compare to the air leakage of wood-stud construction?
2. What characteristics of the houses explain the variability in air leakage within ICF construction?
3. How does this variability affect the energy use of ICF houses when compared to wood-stud construction?

Chapter 2 of this thesis examines previous work done on air leakage of different construction types and their effect on energy use. It presents studies most relevant to the questions above and reveals topics that have not yet been explored.

The goal of Chapter 3 is to investigate the first question, above. First, blower door tests of 43 ICF houses in seven states are conducted. This is larger than any other collection of ICF air leakage data. The resulting set of information consists of infiltration and leakage area data, along with characteristics about each house. Chapter 3 provides an analysis of the trends in this data and the characteristics of the houses that best predict air leakage. This chapter also includes a comparison of the air leakage of ICF houses with an existing data set of conventionally built homes. These are generally assumed to be wood-stud construction.

Chapter 4 more fully explores the variability of the air leakage data introduced in Chapter 3. This process involves examining the leakage sites of two houses from the data set, one that is unusually leaky and the other unusually tight. By understanding where these houses leak and the relative sizes of the holes, the differences between them can be identified. Not only will this explain why there is a range in leakage area of ICF houses, it will establish the important leakage sites as well.

Finally, Chapter 5 will develop an energy simulation of a typical US house. Using the comparison of ICF and wood-stud construction air leakage completed in Chapter 3, reasonable values of air leakage will be input. The results will display how infiltration affects energy use in two different climates, Chicago and Phoenix.

Chapter 6 will identify the primary conclusions of this thesis and their importance.

1.5 Summary

This introduction identifies the importance of energy use in single-family residential houses. It also motivates the roles air leakage and insulated concrete form have in the discussion. Finally, the three main questions of this thesis and how they will be answered are presented.

2. Literature Review

2.1 Introduction

This chapter reviews previous work done on air leakage and insulated concrete form houses. It begins with a review of the definitions, physics and quantification of air leakage. Then, literature on concrete structures, leakage sites and how infiltration affects energy use will be summarized. This will guide the work towards the final goal of understanding the air leakage of insulated concrete form houses, its uncertainty, and its effect on energy use.

2.2 Basics of air leakage

Air leakage, or infiltration, is the movement of air in and out of a house through unplanned openings (Sherman and Chan, 2004). Because this air must be heated or cooled, this phenomenon can cause a large amount of unnecessary energy use. According to Shaw et al. (1973), air leakage depends on wall design, materials used, workmanship, and the condition of joints.

Pressure differences between the indoors and outdoors induce infiltration. The most common method of estimating the volumetric airflow rate through a building is seen in Equation 2-1, which is a generalized form of the orifice equation.

$$Q = c\Delta P^{n} \qquad (2\text{-}1)$$

where

Q = the volume flow rate, m^3/s

c = the flow coefficient, $m^3/s/Pa$

ΔP = the indoor/outdoor pressure difference, Pascals

n = the pressure exponent, dimensionless

There are two weather phenomena that can create this pressure difference: temperature and wind. Air temperature determines changes in air pressure with height, so a temperature difference between indoor and outdoor air can create a pressure differential, which drives infiltration. In addition, the wind can change the pressure on the outside of a building positively or negatively, depending on building and wind characteristics (ASHRAE Fundamentals, 2009).

The value of n is based on the type and properties of the opening. If the Bernoulli equation is used, which assumes the leak has a short path and frictional forces can be ignored, n = 0.5. This value is used if there is a high Reynolds number because inertial forces are much greater than viscous forces. If the flow rate is low, there will be losses due to friction. This causes the flow rate to be linearly proportional to the pressure and therefore n = 1.0. Generally, n is found to be at a value in between 0.5 and 1.0 (Sherman and Chan, 2004).

The most common method of air leakage measurement is fan pressurization, when a fan installed in a doorway creates a uniform pressure across a building envelope. There are three different methods of fan pressurization: create several different pressures and measure the flow of air through the fan at each; create a volume change on the inside of a building and measure the pressure response (AC pressurization); provide one pressure pulse to the building and view the decay (pulse pressurization) (Sherman and Chan, 2004).

The first method is the most common, and will be the only one addressed and used in this research. ASTM E779 describes how to determine air leakage from these measurements (ASTM, 2003). This procedure, summarized below, quantifies infiltration in two ways: flow and leakage area. Flow is the volume of air flowing through the holes in the outer envelope when the home is at a specified pressure difference. Generally, the infiltration is reported at a pressure difference of either 50 Pascals, where an accurate reading can be made, or extrapolated to 4 Pa, which is a typical condition. It is generally reported in m^3/s. Leakage area is the size of the holes in the outer envelope of a building, typically in units of cm^2. The procedure to determine the volume flow rate and the leakage area is:

1. Install a fan in the doorway and increase the pressure in a house from 10 to 60 Pascals in steps of 5 or 10 Pa. Measure the flow through the fan at each pressure.
2. Correct the airflow for the difference in outside and inside density.
    a. Inside and outside temperature and elevation are necessary for this calculation.
3. Take the natural log of both the pressure and the corrected airflow.
4. Calculate the variance in these two sets of data and the covariance of both sets.
5. The exponent in the orifice equation described above, n, is the covariance divided by the variance of the natural log of pressure.
6. Calculate c, according to Equation 2-2:

$$c = e^{\overline{\ln(flow)} - n * \overline{\ln(pressure)}} \tag{2-2}$$

7. Correct c for the difference in indoor and a reference viscosity.
8. Calculate leakage area using Equation 2-3:

$$A_L = C_0 * \sqrt{\frac{P_0}{2}} * 4^{n-.5} \tag{2-3}$$

Every house has a different value of volume flow rate and leakage area. Because these houses have some differing attributes that may contribute to the difference in air leakage, it is typical to normalize by these characteristics. For example, the most common way to normalize volume flow rate is to divide it by house volume. This eliminates the effect the difference in house volume has on leakage area – a larger house would intuitively have a larger envelope and therefore more leakage sites – and the resulting numbers can be compared without considering this difference.

When flow rate is divided by house volume, a metric known as air changes per hour is found, as seen in Equation 2-4. Essentially, the number of air changes per hour is how many times, in one hour, all of the air in a house is turned over and replaced by outside air.

$$ACH = \frac{Q}{Volume} * \frac{3600s}{hour} \tag{2-4}$$

where
ACH = air changes per hour, h^{-1}
Q = flow, m^3/s

Floor area and surface area can both be used to normalize leakage area. The most common method is seen in Equation 2-5, where both attributes are used.

$$NL = 1000 * \frac{A_L}{A_f}\left(\frac{H}{2.5m}\right)^{0.3} \tag{2-5}$$

where
NL = Normalized Leakage, dimensionless
A_L = Leakage area, cm^2
A_f = Floor Area, m^2
H = Height, m

Although the leakage area is a property of a building, the flow rate varies with temperature and wind speed. In order to calculate flow from leakage area without experimental results, Sherman and Grimsrud developed an equation in 1980, separating temperature from wind effects. This can be seen in Equation 2-6 (Sherman and Grimsrud, 1980).

$$Q = \frac{A_L}{1000} * \sqrt{C_S \Delta t + C_W U^2} \tag{2-6}$$

This equation uses the leakage area, A_L, the temperature difference, and the wind speed to calculate flow rate. In addition, the stack coefficient, C_S, is based on the height of the house and the wind coefficient, C_W, is derived from height and shelter class. This equation is commonly used in energy modeling, when temperature and wind speed are input every hour in order to achieve more accurate results. A similar, although slightly more complex, version is used in this thesis and will be introduced in Section 5.3. According to Al-Homoud (2004), in addition to temperature differentials and wind velocity, infiltration depends on tightness of construction, exterior shielding, and building height. Therefore, Equation 2-6 captures all of the elements that lead to airflow.

2.3 Infiltration of concrete structures

Persily et al. (2006) completed the most recent analysis of the largest set of air infiltration data in the United States: the Lawrence Berkeley National Laboratory database. They then calculated representative values of normalized leakage, which can be seen in Table 2-1. These values are for houses across the US, and therefore are generally wood-stud construction (Persily, 2006). This is a very complete analysis and should represent typical houses. However, they did not consider how different types of envelopes may affect the air leakage of a house.

Table 2-1. Representative values of normalized leakage based on the LBNL database (from Persily (2006) Table 5)

	Normalized Leakage Area (dimensionless)	
Year Built	Floor area less than 148.6 m^2 (1600 ft^2)	Floor area more than 148.6 m^2 (1600 ft^2)
Before 1940	1.29	0.58
1940-1969	1.03	0.49
1979-1989	0.65	0.36
1990 and newer	0.31	0.24

Becker (2010) compares different types of concrete walls for their air tightness. He finds that autoclaved aerated concrete block walls are tight when compared to regular and lightweight aggregate concrete block walls. However, a layer of lime-cement coating can reduce the air changes per hour significantly. Although this is a reasonable conclusion, it does not deal with insulated concrete form, the envelope this thesis examines, nor does it examine non-cementitious options.

Several studies compare concrete buildings with other building types. This thesis will primarily focus on studies in the United States. Shaw et al. (1973) find that tile and plaster walls are generally more leaky than concrete and steel, but that concrete and steel do not seem to differ greatly. Persily (1999) concludes that frame and masonry buildings may be slightly leakier than concrete, panel, manufactured, metal and curtain wall envelopes. Although these conclusions are valid, these studies do not examine insulated concrete form envelopes.

Kosny et al. (1998) references a study by Southwest Infrared Inc., which states that blower door tests of 7 ICF houses show that ICF houses are inherently tighter. This study was not available online, through the MIT libraries, or from the author. However, a dataset consisting of seven points seems quite small to make any conclusion about tightness. It is not clear if these houses are similar in design, in the same climate zone, or the same age. However, Kosny et al. use the air tightness found for the ICF houses and then a 20% larger value for wood homes. This is a large assumption given the small size of the data set.

On a more specific level, Petrie et al. (2002) observe two side-by-side homes, one made from ICF and one built from a wood frame. They compare them using flow rates from blower door testing. On average, the ICF house leaks 0.345 m^3/s and the conventional house leaks 0.390 m^3/s. Therefore, there is typically a difference of 0.045 m^3/s at 50 Pa. To put this in perspective, using a standard house floor area of 222 m^2 times 3 m in height, the passivhaus standard of .6 ACH at 50 Pa, which is considered very low, allows 0.111 m^3/s. The difference between ICF and wood found by Petrie can now be considered quite small, which is a legitimate result. The authors attempt to account for variation in the data by redoing the blower door tests in reverse order. There is no process of understanding how ICF houses can vary by construction crew, climates, or age, for example.

Several studies have also found that infiltration does not vary based on wall construction. Shaw and Jones (1979) concludes that wall constructions do not correlate with differences in air leakage. In addition, in his master's thesis, Doebber (2004) describes the large amount of controversy related to this topic. Although he does assume that the standard normalized leakage value for wood-framed houses is lower than the one for concrete homes, 1.21 versus 0.76, he is unsure if this assumption is legitimate. There does not seem to be any study that examines a large data set, understands its variability, and reaches a strong conclusion on the air leakage of ICF compared to wood frame houses.

2.4 Air leakage variability

In this thesis, the study of variability is generally connected to the study of leakage sites. Differences in air leakage are typically attributed to differences in location or size of leakage sites.

There is a body of literature on where leaks occur and their size. One study by Kalamees et al. (2008) does a blower door test and then uses infrared imaging to see where the air is leaking on several different buildings (2008). However, they only use the results to identify typical locations, as opposed to comparing the variability among the buildings.

Nagda et al. (1986) constructs two identically leaky homes and retrofits one of them. However, he does this by purposely omitting 11 different typical methods of tight construction. This is not realistic and only captures the tightening of purposely-leaky sites as opposed to typically leaky sites. He is able to reduce the air leakage by approximately 35% through retrofitting. Although this shows that retrofitting can be useful, it does not teach the audience about unknown leakage sites.

Another idea used in several studies is sequential blower door testing. Nabinger and Persily (2011), Gammage et al. (1986), and Gettings (1988) all perform blower door testing, retrofit the building and then blower door test again to determine the contribution of the leakage sites to air infiltration. Nabinger and Persily (2011) install house wrap and fix leaks in the floor, Gammage et al. (1986) investigate the ductwork, and Gettings (1988) caulks, adds weatherstripping, installs door jambs/sweeps and seals other locations with foam and tape. Although the results exhibit the contribution of these locations, the studies either do not distinguish among the different types of retrofits - they perform them at the same time and do a blower door test after they have all been completed - or only examine one component such as ductwork.

Dickerhoff et al. (1982), Bassett (1986) and Armstrong et al. (1996) use a similar method and separate the different possible leakage sites to understand how much each contributes to the total leakage. For example, Dickerhoff et al. (1982) measures 34 houses in Atlanta, Georgia, Reno, Nevada and San Francisco, California. Based on these homes, they find that ductwork, electric gaskets, the fireplace, the kitchen exhaust vents and the bathroom exhaust vents contribute 13%, 1%, 24%, 6% and 3%, respectively, to the air leakage. In addition, there is a collection of study results in ASHRAE (The American Society of Heating, Refrigerating and Air-Conditioning Engineers) Fundamentals (2009). A summary of leakage contributions, which will be further discussed in Chapter 4, is:

- Walls: 35%
  - This includes cracks between components such as top plates, outlets, and plumbing penetrations
- Ceiling details: 18%
  - Including recessed lighting
- HVAC systems: 18%
- Fireplaces: 12%
- Vents: 5%
- Diffusion through walls: <1%

Again, although interesting, these results do not compare different types of buildings. There is a lot more that can be learned from the data collected for this summary.

Finally, there is a large collection of air leakage contributions of individual components. Each part of a building has a leakage associated with it. A comprehensive list can be found in the master's thesis by Frye (2011). Reinhold and Sonderegger (1983) uses this type of data and shows very good agreement between leakage area determined by summing components and the whole house blower door test results.

The idea that the number of leakage sites can account for differences in total leakage is similar to the approach taken in this thesis. In Chapter 4, differences in the type and number of leakage sites are compared to explain uncertainty in air leakage.

2.5 How infiltration affects energy use

2.5.1. Percent of energy consumption due to infiltration

Shaw and Jones (1979) finds that 29% of heating loads are due to air infiltration based on a survey of 11 schools. Sherman (1985) states that approximately one third of energy use is due to infiltration. VanBronkhorst (1995) reports based on a study of 25 office buildings that 15% of heating load consumption is due to infiltration, while cooling requirements do not depend on air leakage. Finally, Emmerich and Persily (1998) find that between 16 and 29% of heating and cooling loads are due to infiltration. This paper also investigated 25 office buildings. Unfortunately, the wide breath of types and quantities of buildings studied makes it difficult to come to a unique number. In addition, these results are all from data. It would be interesting to understand how much influence infiltration has when using energy modeling for a typical building. This is discussed further in Section 2.5.3, where there is a review of studies on changes in energy use due to air leakage, some of which use energy models.

2.5.2. Percent of energy loss due to infiltration

Another way studies report their findings is the percent of energy lost due to infiltration. This may be the same statistic as discussed above, if it is assumed that the occupants make up for the energy lost by consuming more. However, if their home is simply colder or warmer, this may not be the case. Tamura and Shaw (1977) find that infiltration causes between 22 and 46% of heat loss (1977). Balaras et al. (1999) find that between 7 and 25% of heat loss is due to infiltration (1999). Overall, these statistics are somewhat similar to the energy consumption numbers above and do not include energy models.

2.5.3. Changes in energy use due to infiltration

There are several studies that report the change in energy use due to changes in infiltration. First, Emmerich et al. (2005) reduce infiltration from 0.17 - 0.26 to 0.02 - .05 air changes per hour on a two-story office building, a one-story retail building and a four-story apartment building in an energy simulation. This is an 83% reduction, on average. They find a 40% energy savings for gas use and a 25% energy savings for electricity use. Although these results are reasonable, this study does not examine single-family houses, which are the topic of this thesis.

Purdy et al. (2001) increase the infiltration from 1.5 to 3 air changes per hour in a simulation of a specific house, and observe a 27% increase in the heating load. However, the house modeled represents a typical energy efficient house in Canada. This does not further our understanding of conventional US homes.

In a study mentioned above, Kosny et al. (1998) use a smaller infiltration rate when simulating typical ICF and stud houses. They find that a reduction of infiltration by 20% in an ICF home causes a heating and cooling energy reduction of 4% in Miami and 6.5% in Washington D.C. As discussed above, this assumption is based on a dataset of 7 houses, which is small for any substantial conclusions.

Petrie (2002), also discussed above, finds that ICF construction is less leaky than wood-stud by comparing two in-situ houses using blower door testing. The only other difference between these homes is the thermal resistance, because ICF construction has a slightly greater R-value. By monitoring them for 11 months without occupation but on a simple operating schedule, it is found that the ICF house uses 5.5% - 8.5% less energy. However, because the houses differed in both leakiness and conductivity, the difference in energy use cannot be solely attributed to air infiltration differences.

Finally, Nabinger and Persily (2011) reduce the air leakage by 18% in a single, unoccupied manufactured house through retrofits. They note an energy consumption drop for heating and cooling of 10%. However, this is not a typical US house.

As seen in all of the above examples, whether based on simulation or monitoring, reduction in infiltration can cause a significant drop in energy consumption. However, none of the studies use the simulation of a typical US house with values of air leakage that are based on substantial evidence.

2.6 Conclusions

This chapter finds that:

1. There is currently no study that compares the air leakage of a large collection of ICF and wood-stud construction single-family houses.
2. Although there has been research done on leakage sites, no study uses this information to understand variability among houses with different types of envelopes.
3. Many papers examine the energy associated with infiltration, but none use the simulation of a typical US house with justifiable values of air leakage.

These findings directly relate to the questions introduced in Chapter 1. This thesis will add to our understanding of each of these aspects of air leakage and energy in Chapters 3, 4 and 5, respectively.

3. The Air Leakage of Insulated Concrete Form Houses

3.1 Introduction

As seen in the literature review, extensive research has been done on the air leakage of houses. The leakage of different construction materials has also been compared. However, there does not appear to be any previous examination of a large collection of insulated concrete form houses. Comparing two houses can be useful, but this lacks consideration towards variability. This chapter presents new results on:

1. A collection of blower door tests and characteristics of ICF houses
2. An examination of the trends in this data including its distribution, variability, and characteristics which best predict air leakage
3. A comparison of the ICF air leakage data to the air leakage of conventional US houses, which are generally considered to be wood-stud construction

3.2 Experimental results from blower door testing

To address the lack of information on the air leakage of ICF houses, blower door tests were conducted on 43 ICF houses. Data was also collected on characteristics of the houses. The purpose of this section is to understand what data is collected, and then organize, categorize and visualize it. The code written for this analysis can be found in Appendix A.

3.2.1 Methodology

The blower door tests include information on the following items. These are based on the survey form found in Appendix B.

- Flows and pressures, with the ducts both opened and closed
- The temperature, before and after the test, both indoors and outdoors
- House geometry
  - Volume
  - Floor area
  - Height
  - Perimeter measurements
- Window and door size and number
- The HVAC system
  - Type
  - Supplies and exhausts
- Location and year built
- The consultant who performed the test
- The leakage area, CFM at 50 Pascals, and ACH reported by the consultant

The locations and distributions of the collected dataset can be seen in Figure 3.1. Although the set does not have a large geographic range, the number of data points is considered satisfactory for analysis.

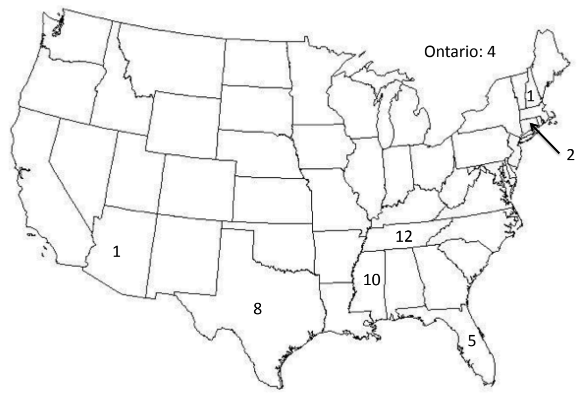

Figure 3.1 The location and distribution of the data collected on insulated concrete form houses is large enough for analysis.

In total, there were 43 tests conducted in seven states. However, three of these are removed because they do not include the original flow and pressure measurements, including one from Arizona, New Hampshire and Ontario. In addition, ten tests in Mississippi measure a set of attached row houses. These homes are very similar in results, as though one house was sampled many times. Because there are only 30 other points, the dataset appears to favor this specific leakage area. This is considered unsatisfactory, and only one of these ten points is left in the data set; the median is selected. These ten points will be explored later in this chapter to understand the variation due to quality control of the builder and random variation. The final number of data points is 31.

Using the flows and pressures, ASTM E779 Standard is used for each house to calculate a leakage area. Appendix C contains the results, as well as the height and floor area of each house.

3.2.2 Results

The histogram in Figure 3.2 on the left includes the leakage area data for all 43 houses, in centimeters squared. The histogram on the right in Figure 3.2 is the air leakage data with 12 tests removed, as described above. The x-axis displays the center values of the bins and the values above the bars are the number of data points in that bin.

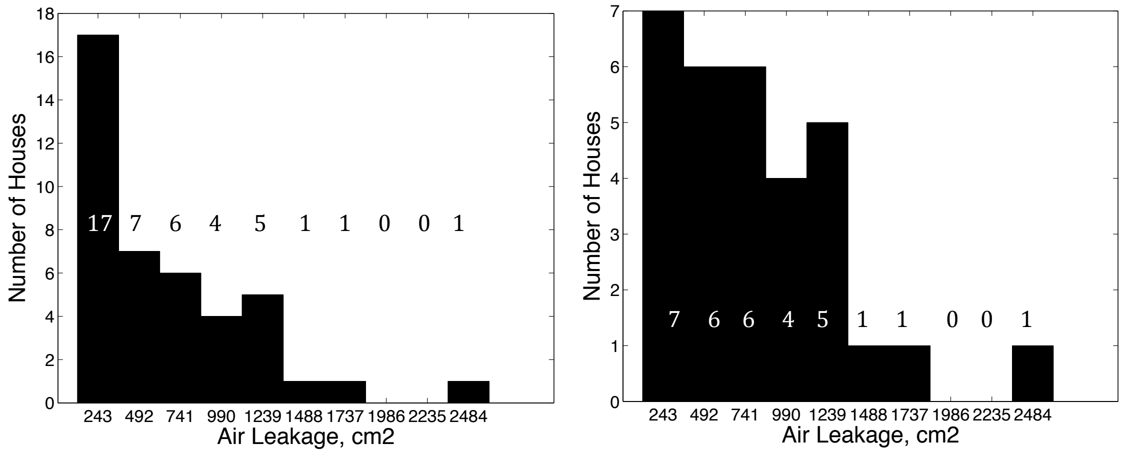

Figure 3.2. The histogram of air leakage of all the houses (left) and the histogram of the final 31 houses (right) display that air leakage of ICF houses favors the lower end of the range.

3.2.3 Discussion

For both charts in Figure 3.2, the numbers favor the lower end of the range. The average value of the 31 points in Figure 3.2 (right) is 793 cm^2. There are few houses at the upper end of the air leakage spectrum.

The house with the very large air leakage does not seem to have any unusual attributes. There may have been some problem in conducting the test. For example, if a window is open, the amount of air leakage during the test might be very large.

3.3 Leakage distribution

It is considered important to explore the distribution of the data for several reasons. First, a large aspect of this thesis is comparing ICF leakage to the US housing stock. In order to understand their relationship, it is necessary to compare their distributions. In addition, by examining the distribution, the variability of the ICF air leakage is scrutinized. Because the ultimate goal of understanding the air leakage is controlling it, the variability is important. Another aspect of this work that adds to the understanding of variability is the analysis of the duct air leakage. It will be shown that the overall variability of the data is demonstrated in this analysis. Finally, in Chapter 5 of this thesis, the energy use of ICF houses is quantified for different leakage areas. In order to use representative values of leakage area, the distribution of the data must be understood.

3.3.1 Methodology

The first task is to determine the distribution of the data. The method of maximum likelihood is employed to calculate the parameters of the most fitting distribution, which is hypothesized based on a visual inspection (Rice, 2007) (Matlab, 2011). These results are compared with the original values using the Kolmogorov-Smirnov test, which determines, non-parametrically, if two datasets are statistically different (Stephens, 1974) (Matlab, 2011). Using a non-parameteric test is important because a t-test, for example, assumes a normal distribution. Then, the parameters found are used to randomly generate a PDF, which can be visually compared to the data itself.

There are three methods for understanding the variability of the data. First, the data is bootstrapped – random samples are taken – and the mean is taken of each sample. The spread of these means indicates how variable the data is and how affected it is by outliers (Rice, 2007). Second, as part of the ASTM standard to calculate air leakage, the method of determining uncertainty is reported. For example, each air leakage is a number plus or minus its uncertainty. A summary of this method can be found in Appendix D (ASTM E779).

Finally, using the series of row houses removed from the data set, the range in air leakage of houses with all of the same measured characteristics can be calculated. This range is due to a combination of the quality control of the builder and random variation of quantities that are not measured in this dataset.

The code written for this analysis can be found in Appendix E.

3.3.2 Results: The distribution and variability

Based on a visual inspection of the histogram in Figure 3.2, the parameters of a gamma distribution are calculated using the method of maximum likelihood to describe the data. For the gamma distribution, Matlab uses the PDF found in Equation 3-1.

$$y = f(x \mid a,b) = \frac{1}{b^a \Gamma(a)} x^{a-1} e^{\frac{-x}{b}} \tag{3-1}$$

The parameters *a* and *b* for the data in this study are 2.38 and 333.79, respectively. At the 5% significance level, this gamma distribution describes the experimental data well. Figure 3.3 displays an overlay of the gamma distribution, created using the parameters found above, on the data.

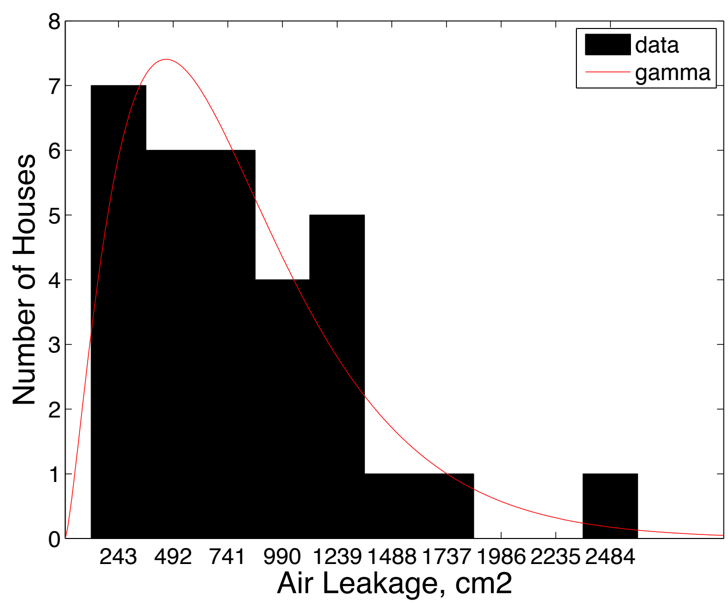

Figure 3.3. A histogram of the air leakage with a gamma distribution overlaid. The gamma distribution has parameters *a* = 2.38 and *b* = 333.8 and is a good fit for the ICF air leakage data.

The next step is to understand the variability of the data. Using the 31 data points being analyzed, the range in leakage area is 2500 cm^2. However, there is one leaky outlier in the leakage area data, based on Matlab's default definition of an outlier. This definition uses the quartile range and a constant multiplier. The multiplier is based loosely on a normal distribution. However, Walpole et al. (2007) state that the constant used by Matlab is typically applied to any box and whisker plot. Therefore this outlier can be removed to achieve a range in leakage area of 1514 cm^2, with a mean of 732 cm^2.

However, this does not explore all the methods of examining variability at our disposal nor does this indicate any of the causes of variability. The following discussion describes the results of three methods of understanding the variability in the air leakage data.

First, the data itself is bootstrapped, and the mean is calculated of each sample. The histogram can be seen in Figure 3.4 and displays a range of 800 cm^2.

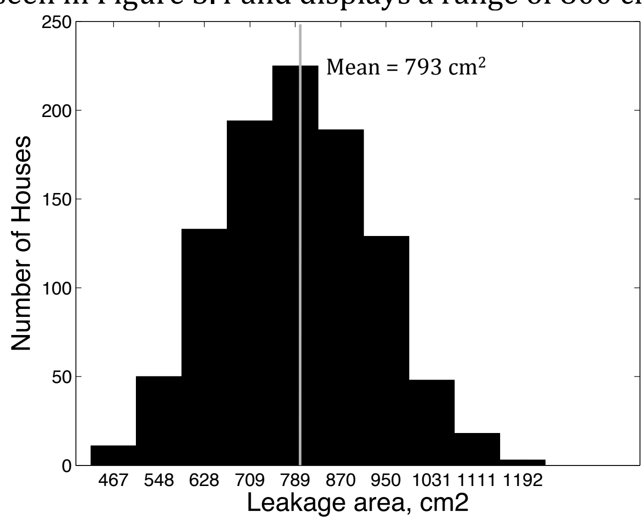

Figure 3.4 The means of samples from the dataset are in groups of ten, taken 1000 times. The mean of all the data, 793, is in the middle of the distribution with variability of approximately 400 cm^2.

The second method is through the ASTM E779 standard, which describes a process for calculating the uncertainty of air leakage, as discussed in Appendix D. The chart in Figure 3.5 displays a histogram of all of the uncertainties. In general, these values are smaller than 300 cm^2.

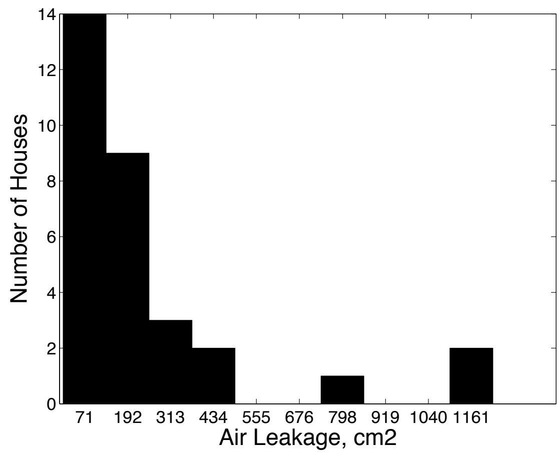

Figure 3.5 In general, the uncertainty of the air leakage based on the procedure in ASTM E779 is lower than 300 cm^2.

The last method for determining variability is based on the fact that there are blower door tests of ten row houses, as discussed above. The range of these houses is 80 cm^2, with an average air leakage of 229.2 cm^2.

A final component of the blower door tests is that several of the tests are taken with the ducts opened and closed, using duct masking to manually cover the ducts. Ducts contribute to air leakage because they typically run to an un-conditioned space where the equipment is stored and leak air into these spaces. Duct air leakage has been shown to greatly contribute to overall leakage (Gammage, 1986) and this is an excellent way to understand how much air leakage they contribute in the ICF dataset. A plot of air leakage for each house when the ducts are open minus the air leakage when they are closed can be seen in Figure 3.6. Based on Figure 3.6, the difference typically fluctuates between plus and minus 50 cm^2. This fluctuation is an aspect of variability, which will be discussed below. The three outliers will also be examined.

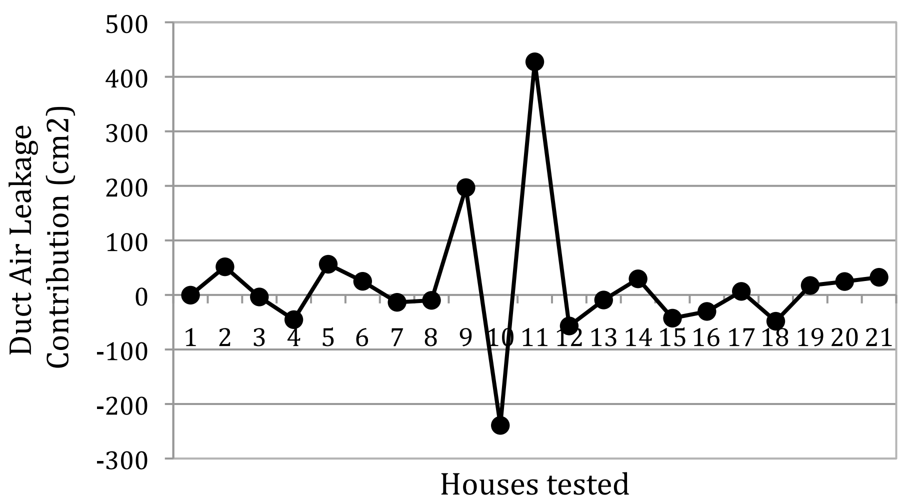

Figure 3.6. Air leakage when the ducts are open minus air leakage when they are closed shows the difference is generally oscillating between plus and minus 50 cm^2.

3.3.3 Discussion: The distribution and variability

Based on a visual inspection and verification, the air leakage data resembles a gamma distribution. This indicates that houses tend towards a smaller leakage area, and that greater leakage areas are less likely. It is encouraging that this distribution resembles that found by Sherman and Matson (2002) for houses across the United States, not necessarily built from ICF. This is evidence that the probability density function of US house air leakage resembles a gamma distribution, regardless of construction technique.

The variability of the data is examined in several ways. First, the bootstrapped means are typically 800 ± 400 cm^2; their range is approximately 800 cm^2. Clearly, if the means of random samples can vary by 800 cm^2, this is relatively variable data and not simply affected by one outlier. This could be due to a number of factors such as differences in climate, house geometry and properties, the consultant who performs the test or factors that are not measured in this study.

The uncertainty is also found using the ASTM E779 calculation. The uncertainty resembles a gamma distribution, and is typically ±100 cm^2. The largest uncertainty that does not appear to be an outlier is approximately ±400 cm^2, similar to the variability of the means, discussed above.

Finally, the range in leakage area of a set of row houses is 80 cm^2. However, there are no property differences among these buildings. The builder, climate, floor plans and all other factors are the same. This range is due in part to the quality control of the builder, or in other words, how similarly a crew constructs different houses using the same plan. The range is also caused by random variation. For example, if there is a strong wind that for some reason hits one house more than the others during testing, that house could appear leakier.

The last aspect of the air leakage data is that tests are taken with the ducts both opened and closed. In general, the difference in air leakage when the ducts are open and when they are closed varies between +50 and -50 cm^2. It is expected that leakage with the ducts open would always be greater than that with the ducts closed because the measurement would capture the leakage from the ducts. Therefore, the fact that there are many tests where the leakage decreases when the ducts are open is surprising. This is most likely due to random variation in the data.

There are three outliers in Figure 3.6. These houses do not have unusual characteristics, and the contractor who performed the tests performed others on houses with similar HVAC systems with more reasonable results. The two positive points are either due to error or high duct leakage in those particular houses. The negative point, however, can only be explained via experimental error. The house was examined, and there is no reason why the ducts should increase the tightness of the house. They run to the unconditioned attic, and the HVAC system is not unusual. The house that displays this anomaly – number ten - does have the highest leakage area of all those examined for duct leakage. However, the leakage areas were plotted against the duct leakage and no correlation was found. Leakage area does not influence duct leakage. It might be that a door or window was accidentally left open while the test with the ducts closed was conducted.

3.4 Leakage prediction

3.4.1 Introduction

The purpose of this section is to determine the characteristics of a house that can be used to predict its air leakage. This is a good indication of where the house is leaking, and can increase our understanding of the causes of variability. For example, if a certain characteristic is more important for prediction, perhaps its fluctuation is the cause of the variability in the data.

3.4.2 Methodology

In order to quantify different predictors, many variables are measured, including those in Table 3-1.

Table 3-1. Characteristics of each house measured during the blower door tests, which are considered possible predictors of air leakage

1	Floor area
2	Height
3	Year
4	Number of vents
5	Surface area
6	Volume
7	Climate
8	Number of windows
9	Area of windows
10	Number of doors
11	Area of doors
12	Mechanical ventilation system
13	Which consultant performed the test
14	Uncertainty of the air leakage

Climate is based on zones developed in the literature for ASHRAE conferences (Briggs, 2003).

Of the 31 air leakage points, 21 are chosen randomly as test data. The variables of these 21 points are combined in different ways using the following three methods to determine which combination best predicts air leakage:

1. Selection of terms based on visual inspection
   First, variables are examined individually using histograms. Then, all of the variables are plotted against one another and versus air leakage. Visual inspection is used to predict which terms are related and which would best

estimate air leakage. Using linear regression, several combinations of variables are compared.

2. Stepwise regression
   This method reports the most important variables to the user based on the *p* values from a series of F-tests.
3. Regression trees
   This algorithm optimizes the prediction of air leakage based on a series of yes or no variable values.

These methods are compared by examining the air leakage they predict and the corresponding experimental values of air leakage. First, the Root Mean Squared Prediction Error (RMSPE), seen in Equation 3-2, and the median absolute error, Equation 3-3, are calculated for the test data. They are also calculated using the 10 points of air leakage not in the test data, which are labeled the validation data. After examining the validation test data, it is confirmed that the outlier seen in Figure 3.2 is in this set. Therefore, the RMSPE, which can be greatly affected by outliers, is recalculated for the validation data with that point removed.

$$RMSPE = \sqrt{\frac{\sum_{i=1}^{n}\left(f(x_i) - y_i\right)^2}{n}} \qquad (3\text{-}2)$$

where
f(x) is the fitted data
y is the validation data
n is the number of data points

$$Median\ \ Absolute\ \ Error = Median(abs(errors - median(errors))) \qquad (3\text{-}3)$$

3.4.3 Results
The floor area of the houses is first considered as the most important predictor of leakage area and examined separately as a histogram in Figure 3.7. However, based on the distribution, which is not gamma, it is clear that it cannot predict air leakage alone, and a more complex model is necessary.

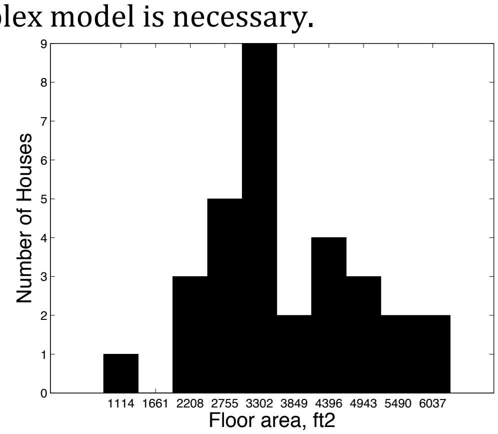

Figure 3.7. The floor area (ft2) of ICF houses does not resemble a gamma distribution, indicating that other predictors are important and must be explored.

Equations 3-4 and 3-5 were created based on visual inspection of other variables.

$$B0 + B1 * volume + B2 * window\_area = leakage\_area \quad (3\text{-}4)$$

$$B0 + B1 * surface\_area + B2 * window\_area = leakage\_area \quad (3\text{-}5)$$

Using stepwise regression, volume is the only characteristic necessary to best predict air leakage. Finally, using the regression tree approach, window area and the presence of mechanical ventilation are the most important characteristics for air leakage prediction.

The details of this analysis can be found in Appendix F. The variables that are determined to predict air leakage best are considered most important. This result begins the discussion of the causes of variability, which will be explored in greater depth in Chapter 4.

Table 3-2 presents all of the different values of error calculated for these four possible methods.

Table 3-2. Different errors calculated for the four different methods of predicting air leakage.

	RMSPE (cm^2)	RMSPE_validation data (cm^2)		Median error_validation data (cm^2)
		With outlier	Without outlier	
Equation 3-4	354	556	151	164
Equation 3-5	340	1100	129	234
Stepwise regression	346	454	200	226
Regression tree	215	517	223	188

If RMSPE is used to select the best prediction method, the regression tree approach would be chosen. If it was the RMSPE of the validation data with the outlier, stepwise regression is the best. Without the outlier, Equation 3-4 has the lowest error. Finally, if the median error is used to decide, Equation 3-5 would be chosen. There clearly needs to be a reason for selecting one error calculation method over another.

3.4.4 Discussion

Several approaches are taken to determine which characteristics best predict air leakage. These include testing sets of variables based on apparent correlation, stepwise regression and regression trees. Different techniques are employed because it is important to determine the most accurate answer and many methods are available. The results are compared using root mean squared prediction error and median absolute error. The RMSPE is calculated both with and without the outlier in the validation data.

It was determined that the best measure would be median absolute error for the following reason. If RMSPE is used with the outlier, that specific data point has a large influence on the result. Because another outlier could easily be calculated in future tests, removing it did not seem reasonable. Therefore, median absolute error can compare the results of the three approaches without being very affected by the outliers or ignoring them.

Equation 3-4 is chosen as the best method of prediction, making volume and window area the most important characteristics. Using linear regression, the coefficients can be seen in Equation 3-6.

$$Air\ \ Leakage = 193.0 + 6.8e - 5 * volume + 0.128 * window\ area \qquad (3\text{-}6)$$

where
Volume is in m^3
Window area is in m^2
Air leakage is in cm^2

The fact that this equation uses volume and area of windows is significant. Volume is a very good measure of how large a house is and how much air it contains. In addition, of all the leakage pathways measured, window area is the most important. Of course, there are many leakage pathways that were not measured, such as rim joist length, soffit vent area or recessed lights. These could be very important, and are more closely examined in the next chapter of this thesis.

3.5 ICF compared to US houses

This section examines how ICF houses compare in air leakage to new, typical houses. This is the first time this has been done with large datasets as opposed to comparing two side-by-side homes or models with assumptions about air leakage.

3.5.1 Methodology

Many measurements have been made on the United States housing stock to determine typical air leakage. This thesis will focus on those that discuss normalized leakage. There is a large database of blower door tests collected by the Lawrence Berkeley National Laboratory (LBNL, Residential Building Systems). Of these homes, 3500 are chosen by Chan et al. (2003) to represent conventional houses. Persily et al. (2006) complete the most recent analysis of this database and use normalized leakage to report the results. Sherman and Matson (2002) have also published their calculation of average normalized leakage. Finally, a published standard, ASHRAE 119 (2004), reports a recommendation for normalized leakage of residential buildings. The new data collected on ICF houses for this study is first converted to normalized leakage and then compared to all of these results. In general, because the data is non-normal, values related to the median, rather than the mean, are employed for the comparisons.

The code used for this analysis can be found in Appendix G.

3.5.2 Results

As discussed above, LBNL has compiled a database of blower door tests on 70,000 houses (Chan, 2005). The geographic distribution of these can be seen in Figure 3.8.

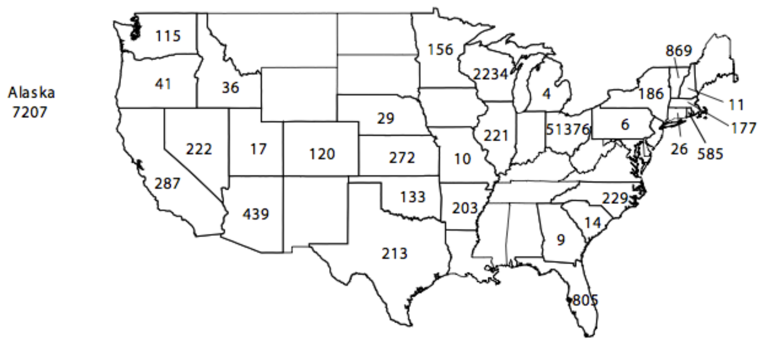

Figure 3.8. Geographic distribution of the LBNL data is well spread although some states have many more points than others (after Chan (2005) Figure 1).

Chan (2005) organizes conventional houses, which do not include low-income or energy-efficient buildings, into Table 3-3. This table first breaks down conventional houses by floor area and then by year built. It reports the number of data points in each category, the geometric mean, the geometric standard deviation, and the 5th, 25th, 50th, 75th and 95th percentiles.

Table 3-3. The normalized leakage of conventional houses that are not participants of low-income or an energy efficiency program (after Chan (2003) Table C5).

Floor Area	Year Built	# Data	GM	GSD	p05	p25	p50	p75	p95
<93 m^2	before 1950	63	1.09	1.84	0.47	0.61	1.09	1.57	3.20
	1950-1979	71	0.98	1.92	0.37	0.60	0.96	1.55	2.88
	1980-1995	29	0.49	1.62	0.17	0.34	0.48	0.74	0.85
	after 1995	17	0.33	1.36		0.28	0.32	0.34	0.48
93-139 m^2	before 1950	166	1.14	1.78	0.37	0.79	1.19	1.53	2.93
	1950-1979	149	0.82	1.73	0.35	0.54	0.82	1.26	2.21
	1980-1995	191	0.44	1.74	0.22	0.30	0.43	0.55	1.11
	after 1995	85	0.34	1.45	0.20	0.28	0.33	0.41	0.61
140-185 m^2	before 1950	149	0.74	1.76	0.33	0.48	0.67	0.95	2.24
	1950-1979	186	0.51	1.68	0.23	0.37	0.49	0.66	1.78
	1980-1995	163	0.41	1.79	0.16	0.27	0.38	0.64	1.05
	after 1995	75	0.28	1.57	0.11	0.23	0.31	0.36	0.47
186-232 m^2	before 1950	200	0.55	1.49	0.31	0.44	0.54	0.69	1.09
	1950-1979	275	0.40	1.49	0.21	0.31	0.39	0.50	0.75
	1980-1995	129	0.35	1.59	0.15	0.27	0.37	0.50	0.74
	after 1995	67	0.25	1.64	0.06	0.21	0.27	0.35	0.43
>232 m^2	before 1950	328	0.53	1.41	0.29	0.44	0.55	0.67	0.89
	1950-1979	543	0.37	1.40	0.21	0.30	0.37	0.46	0.61
	1980-1995	159	0.29	1.67	0.13	0.20	0.30	0.44	0.58
	after 1995	403	0.18	1.68	0.07	0.14	0.19	0.25	0.39

The values in the box are the 50th percentiles, the medians, of normalized leakage for the type of home specified by area and year. Persily (2006) then averages the numbers by year for the floor areas below and above 139 m^2. This produces the chart seen in Figure 3.9.

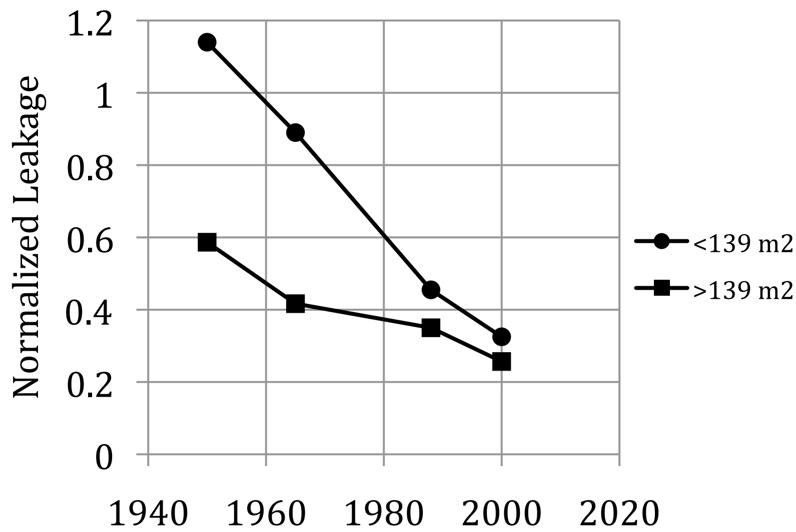

Figure 3.9. Normalized leakage versus year built based on Persily (2006).

In general, these houses are considered wood-stud construction since that is the most prevalent building method in the US housing stock. Therefore, the current study uses the chart in Figure 3.9 to compare the normalized leakage of wood-stud and ICF houses. When examining the ICF house data, the median floor area is 314 m^2. Therefore, the line for US houses smaller than 139 m^2 in Figure 3.9 is removed. In addition, to understand the variability in this analysis, the 5th and 95th percentiles of the most recent point are included. Then, the median, third quartile, first quartile, minimum and maximum of the normalized leakage of the collected ICF data are plotted for the year 2007, the median year the houses are built. This final comparison can be seen in Figure 3.10.

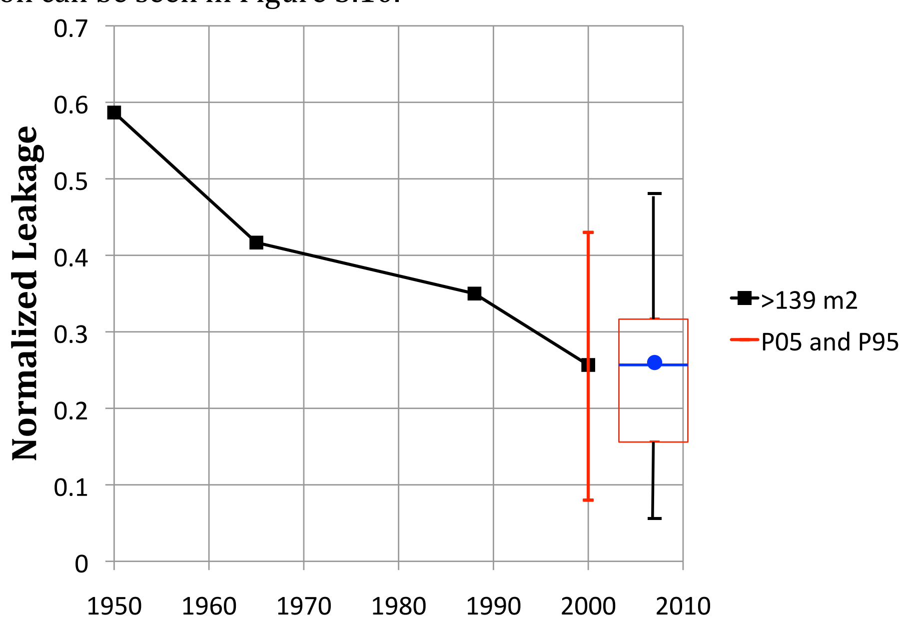

Figure 3.10. Normalized leakage for both the US housing stock and collected ICF house data, with their variability, displays similar normalized leakage of the two types of construction.

Finally, Persily performs a linear regression of the points in Figure 3.9 and calculates the values of normalized leakage in 1940, 1955, 1979, and 1998, approximately. These numbers are reported in Table 3-4.

Table 3-4. Representative values of normalized leakage allow the ICF data to be compared to the US housing stock (from Persily (2006) Table 5).

	Normalized Leakage Area (dimensionless)	
Year Built	Floor area less than 148.6 m^2 (1600 ft^2)	Floor area more than 148.6 m^2 (1600 ft^2)
Before 1940	1.29	0.58
1940-1969	1.03	0.49
1979-1989	0.65	0.36
1990 and newer	0.31	0.24

These values are plotted in Figure 3.11 along with the average normalized leakage found by Sherman and Matson in 2002 and the ASHRAE 119 standard. The box and whisker plot is the ICF data including its median, first and third quartiles, and two outliers.

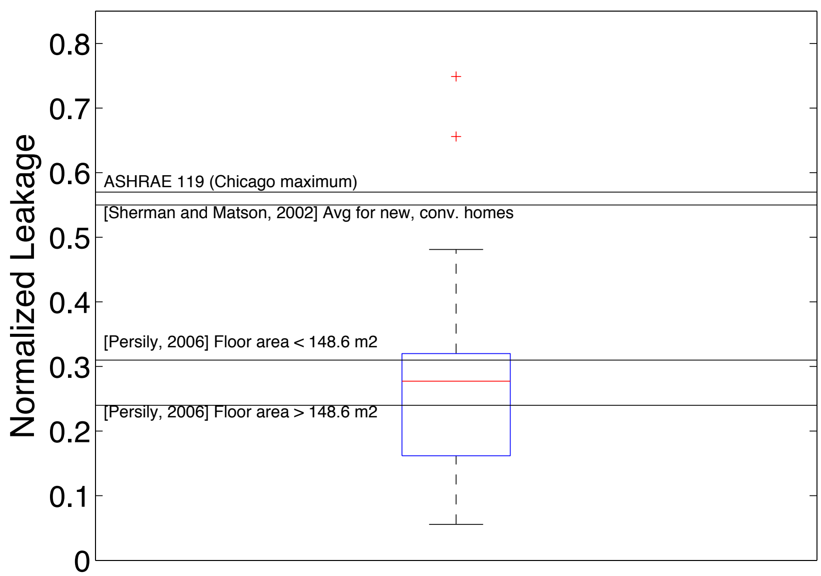

Figure 3.11. Normalized leakage of the ICF data is similar to the most recent analysis by Persily (2006) but smaller than Sherman and Matson's average (2002) and the ASHRAE standard.

3.5.3 Discussion

When comparing the ICF data to Persily's graph in Figure 3.10, it is clear that new wood-stud houses are very similar to new ICF houses. Their medians are almost identical: 0.2599 for the ICF and 0.2567 for the wood data. These are only 1.2% different, and the range of data is similar. It is important to note that this is comparing the 5th and 95th percentiles of the wood houses, as these are the numbers reported, to minimum and maximum of the ICF, because a 5th and 95th percentile would mean very little on a dataset of 31 points. Therefore, the complete range of the wood air leakage might be a bit larger than it appears. Of course, this would simply make the two data sets more similar. These observations motivate the study in the next chapter of this thesis on the reason for the variability of the ICF air leakage data. In addition, when comparing the ICF data to older US houses, ICF normalized leakage is much smaller. This could be because houses are built more tightly. Of course, average house size has increased over time: 1525 ft^2 in 1973 to 2169 ft^2 in 2010 (US Census). Therefore, it may be that houses today have similar leakage areas but are larger.

In terms of the comparison to Sherman and Matson's data point in 2002 and ASHRAE Standard 119, ICF houses are quite tight. One problem with the comparison to ASHRAE Standard 119 is that it was published in 1988, and therefore may be outdated.

3.6 Conclusions

This chapter:

1. Presents the largest dataset of ICF air leakage available to date, based on new blower door tests conducted for 43 houses in the US and Canada.
2. Displays that ICF air leakage tends towards smaller values, that the variability is quite large - 800 cm^2, with a mean of approximately 800 cm^2 – and that volume and window area are the best predictors of air leakage.
3. Finds that the median of ICF normalized leakage is 0.2599 and 0.2567 for wood data. These are 1.2% different.

The next question to address is clearly what is causing the air leakage and why it is so variable. This is discussed in the next chapter of this thesis.

4. The Variability in the Air Leakage of Insulated Concrete Form Houses

4.1 Introduction

As seen in the previous chapter, the range of normalized leakage of the 31 ICF houses sampled is similar to that of the 3500 houses analyzed by Chan et al. in 2003. This large range is surprising and prompts the question as to why insulated concrete form houses of similar construction vary so greatly. It is hypothesized that the difference between a tight house and a loose one is due to a difference in the number of leakage sites or in the leakiness of the sites. In other words, there may be additional leakage sites in the looser house, or the locations of leakage are similar and the looser house simply has larger holes. This chapter describes the approach taken to understand the variability of the air leakage of ICF houses and the resulting conclusions.

In order to test this hypothesis, one loose ICF house and one tight ICF house are examined. The 31 houses tested are in several different locations, and it is important to choose two houses in the same location to eliminate any difference in climate. After examining the leakage of the houses, the largest range in leakage area in a specific location is in Nashville, Tennessee. The contractor who completed the original tests suggested that the tightest house in Nashville, with a leakage area of 494 cm^2, and the second leakiest ICF house in Nashville, with a leakage area of 1633 cm^2, should be revisited, due to concern about the legitimacy of the test of the leakiest house. This range is still larger than any other, and appointments were made to visit these residences in Joelton and College Grove, TN.

On the second visit to these houses, four procedures were carried out:

1. Thermal imaging. An infrared camera can take pictures of surface temperatures. In this study, pictures are taken at typical leakage sites in both houses before and during a blower door test, in order to eliminate conductivity effects. The temperatures at specific points are compared using two different equations. The purpose of this comparison is to understand the leakage pathways and their size in the envelopes of each of the houses.
2. Sequential blower door testing. This process involves performing a blower door test, retrofitting a certain component, and testing again. Nine different retrofits are executed in this study on the loose house, with blower door tests after each. These retrofits target typical leakage locations as well as those deemed important upon examining the house. The ultimate leakage area of the loose house after all of the retrofits are completed is compared with the tight house air leakage. This provides an understanding of the size and location of the leakage sites.
3. Verification. First, major conclusions from the combination of thermal imaging and sequential blower door testing are reached. In order to have confidence in these decisions, they are compared to an overview of results from other studies.
4. Recommendations. General recommendations for air sealing from several sources are reviewed to understand where typical houses leak. Based on the

results of the thermal imaging and sequential blower door testing, more specific recommendations are given for ICF houses.

The following section details this methodology.

4.2 Thermal Imaging

4.2.1. Methodology

In order to compare the amount of leakage at different locations, a thermal imager is employed to visualize temperature. Sometimes called an infrared camera, these tools take pictures of infrared radiation from a surface rather than visible light. The machine in this study is a FLUKE TiR series, which has 160x120 pixels (http://www.fluke.com). A temperature is associated with each pixel.

The drawback of thermal imaging is that it can also capture a difference in conductivity of different locations, rather than infiltration. A surface can appear cold due to high conductivity of materials or because cold, outside air is genuinely leaking into the house. In order to overcome this problem, thermal images are taken before and during a blower door test (Kalamees et al., 2008). The blower door test is set up to depressurize the house, bringing outside air in through cracks. Because these tests were done in November early in the morning, this air was generally cooler than room temperatures. Therefore, if air is leaking into the house, the thermal image during the blower door test displays lower temperatures. The blower door test does not change how much energy the materials conduct.

Throughout testing, indoor and outdoor temperatures are recorded as required by the ASTM E779 process and to understand the temperatures driving air infiltration during the thermal imaging.

The locations that are examined using the above procedure include:

1. Typical windows on the north, south, east and west facades
2. Typical doors on two different facades
3. Indoor attic access, if this exists
4. Indoor basement access, if this exists
5. A typical joint between the wall and roof
6. A typical joint between the foundation and wall, in two locations
7. The rim joists in the lower level of the house
8. The rafters in the attic
9. A typical joint between the external wall and an intermediate floor, if the house is more than one story
10. Kitchen and bathroom exhaust and a supply return register
11. Mechanical penetrations from basement to first floor
12. Recessed lighting

These are derived from important sources of leakage found in the literature and what the contractor recommended based on previous experience (Gettings, 1988) (Dickerhoff et al., 1982).

After the images are taken, they are post-processed in a program called SmartView (Fluke, 2009). This includes changing the indoor temperature based on measurements in the house and editing the emissivity of the object being photographed based on measurements of different surface types from third parties (Electro Optical Industries, 2012) (Engineering Toolbox, 2012) (Infrared Services Inc, 2012). Both of these variables moderately affect the temperatures that the thermal camera captures.

The next step is recording temperatures from the images. First, point temperatures on and near the expected crack location are documented in the images both before and during the blower door test. Then, a box is drawn around the coldest region observed in the second image, during the blower door test. This may or may not be on the expected crack location. A box in the same location is drawn in the first image, before the blower door test. The minimum, average and maximum temperatures in the boxes are documented. These techniques were developed in order to ensure that the expected temperature changes as well as any large temperature changes are recorded.

Two equations are employed in order to quantify the amount of infiltration of each leakage location based on the thermal imaging results. The first is found in a paper by Kalamees et al. (2008), and can be seen in Equation 4-1.

$$\text{Relative Leakage} = \frac{T_{before\ \ blower\ door} - T_{during\ \ blower\ door}}{\Delta T_{outdoor-indoor}} \qquad (4\text{-}1)$$

The average temperatures from the boxes described above are used for the numerator in Equation 4-1. For the denominator, the indoor - outdoor temperature difference changes over the course of the blower door test. The two differences in temperature are averaged for the purpose of the equation. Although this disregards some information, it is necessary for the use of Equation 4-1. Another method, the difference in leakage discussed below, does not average the temperatures but has other drawbacks.

Equation 4-1 can produce a negative relative leakage if the sun influences the temperature of the location. If this is the case, the air leakage is considered minimal because it does not overpower the sun's radiation. An example of numbers generated using Equation 4-1 can be seen in Figure 4.1, for a window on each façade. In this case, there is no clear trend between the loose and tight house. Sometimes the tight house has tighter windows and sometimes it has looser ones.

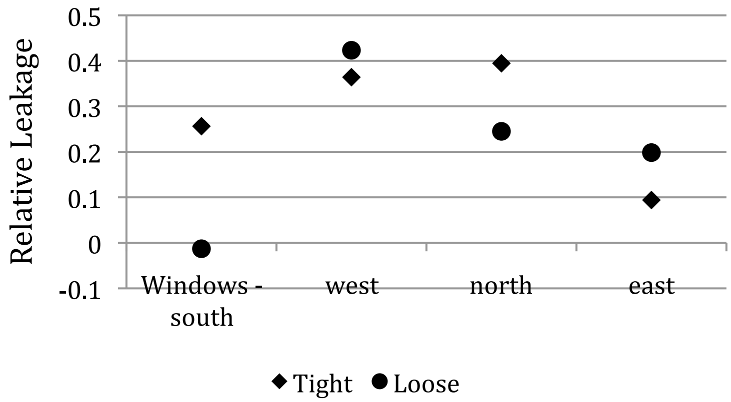

Figure 4.1. The relative leakage of the windows on each facade for both the tight and loose house demonstrates the calculation process and that the values are sometimes slightly negative.

As mentioned previously, another equation was developed in addition to the relative leakage. The problem with Equation 4-1 is that, by averaging the difference in indoor and outdoor temperature for before and after the blower door test, information is lost. In addition, it does not make use of the point temperatures recorded on the expected crack locations as discussed above. Therefore, to account for the changing outdoor temperature and the expected crack location, Equation 4-2 was developed:

$$Difference\ in\ Leakage = \left[\frac{\Delta T_{Twall-Tcrack}}{\Delta T_{inside-outside}}\right]_{before} - \left[\frac{\Delta T_{Twall-Tcrack}}{\Delta T_{inside-outside}}\right]_{during} \quad (4\text{-}2)$$

Each temperature difference between the wall and the crack is divided by the indoor-outdoor temperature difference at the time of the thermal image to normalize it. This is done both before and during the blower door test. The difference between these two numbers is then taken to understand how the blower door changes the temperature at the expected crack location. An example of this equation for the windows in the tight and loose house can be found in Figure 4.2.

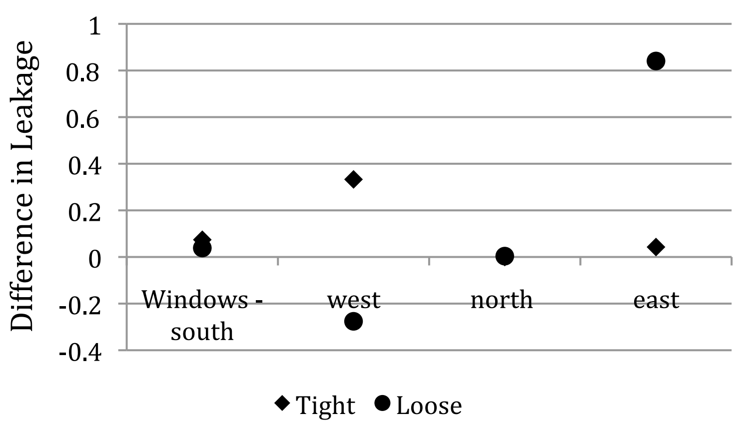

Figure 4.2. The difference in leakage of the windows on each facade for both the tight and loose house demonstrates the calculation process.

Of course, the drawback of Equation 4-2 is that the expected crack location does not always show much leakage. This is reflected in the typically smaller values produced.

4.2.2. Results

First, it was not possible to take an image of all the locations in both houses. The bottom plate is not applicable in the tight house, which will be explained below. The supply register in the tight house was simply too warm to exhibit any leakage. Images of the can lights and plumbing penetrations were not taken at the tight house because they were only considered as possibly important when the loose house was examined, the day after. Finally, he rafters were only measureable in the tight house, because the attic is conditioned and not exposed.

In terms of the images, the expected leakage location is preferably a certain temperature before the blower door test and then the same location becomes colder or remains the same during the test. However, for several of the windows and doors in both houses, the expected leakage location is slightly colder than its surroundings in the first picture, as expected, but either stays the same or becomes warmer – probably due to heat from the sun – in the second image. In addition, most of these pictures show a very cold region during the blower door test in an unexpected location. All of these effects are documented using both the point temperatures on the expected crack locations as well as the boxes around the cold region. These locations can be the same or different.

An example of when the box and points are in the same region is shown in Figure 4.3. The box was drawn in the coldest area in the second image and its respective area in the first. It displays the maximum, average, and minimum temperature within it: 63.3, 60.4 and 57.3˚F before the test and 57.6, 52.8 and 48.4˚F after the test, respectively. Two points, with their temperatures, were drawn on and next to the expected leakage location in both images, as well: 57.1 and 63.1˚F before the test and 53.0 and 58.0˚F after the test, respectively. The color scale is not the same for these images. These images are from the tighter of the two houses.

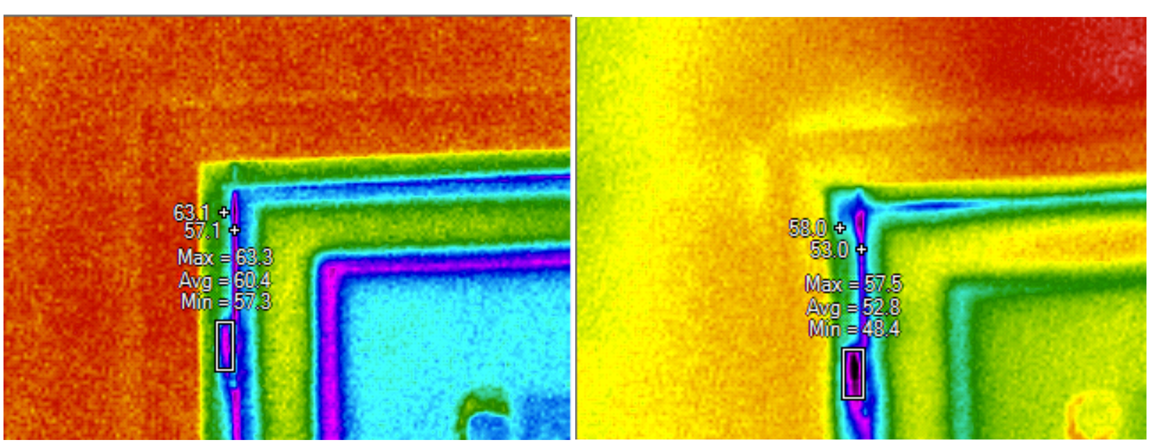

Figure 4.3. Thermal images of the tight house' doorframe, before and during the blower door test. In this instance, the box and points are in a similar location.

An example of the box and points being in different locations can be found Figure 4.4. The box was drawn in the coldest area in the second image and its respective area in the first. It displays the maximum, average, and minimum temperature within it: 64.2, 61.7 and 58.5˚F before the test and 55.2, 52.2 and 49.9˚F after the test, respectively. Two points, with their temperatures, were drawn on and next to the expected leakage location in both images, as well. These temperatures are 61.9 and 68.3˚F before the test and 56.9 and 58.8˚F after the test, respectively. Again, these images are from the tighter house and the color scale is not the same.

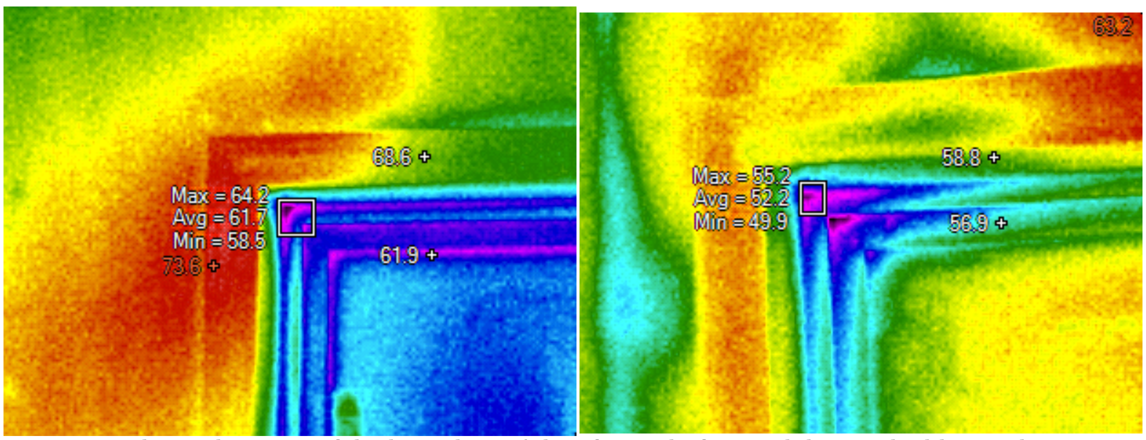

Figure 4.4. Thermal images of the loose house' doorframe, before and during the blower door test. In this instance, the box and points are in a different location.

Based on these results in all the images, the numbers generated using Equation 4-1 can be seen in Figure 4.5.

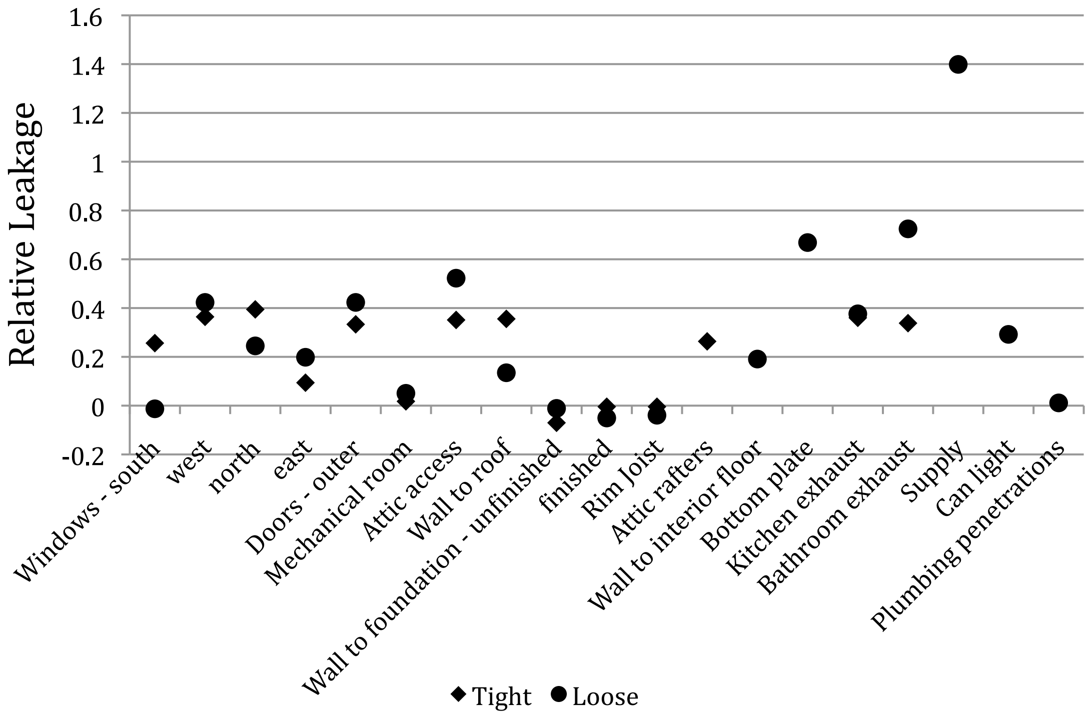

Figure 4.5. The relative leakage contribution of different typical leakage sites in both the tight and loose houses reveals that the largest leakage contributors in the loose house are the bottom plate, exhausts and supplies, and the recessed lighting.

The west window, east window, outer door and attic door have slightly more leakage in the loose house but the north and south window have less leakage in the loose house. The mechanical room door leakage is very similar. Therefore, there is no consistent trend. The wall to roof, wall to foundation, and rim joist connections do not contribute a large amount of leakage for either of the buildings. The rafters seem to contribute a small amount to the leakage in the tight house. The final variables are mostly measured in the loose house. In particular, the bottom plate, supplies, and recessed lighting contribute to the air leakage. The exhausts are measured in the tight and loose houses and contribute to the leakage in both, although much more so in the loose house for the bathroom exhaust.

To understand what the bottom plate is, it is important to understand how the loose house is constructed. First, it can be viewed as a one-story home. However, the roof is built at a very steep angle and two bedrooms are inserted into it. Therefore, the bedrooms are on the same level as the attic. The bottom plate, which connects to the lower part of the stud, may cause leakage from the house into the unconditioned attic. A schematic of this layout can be seen in Figure 4.6. Based on this analysis, the bottom plate is an important aspect of the leakage.

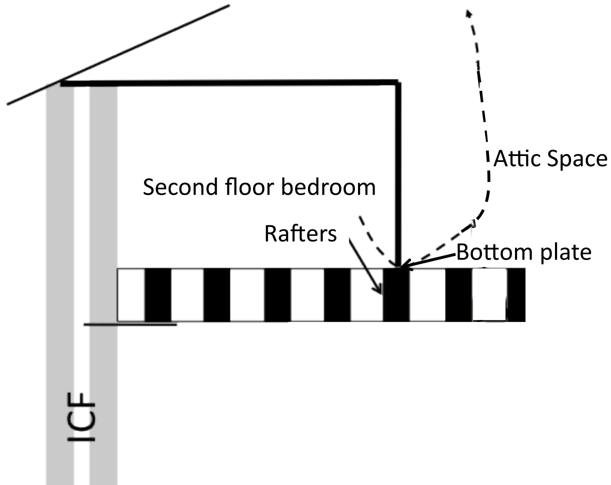

Figure 4.6. A schematic section view of the loose house displays that the second story is on the same level as the attic.

Finally, the exhaust and supply vents and the recessed lights seem to contribute to the air leakage. The lights are examined using sequential blower door testing, discussed below, as well.

The numbers generated using Equation 4-2 can be seen in Figure 4.7.

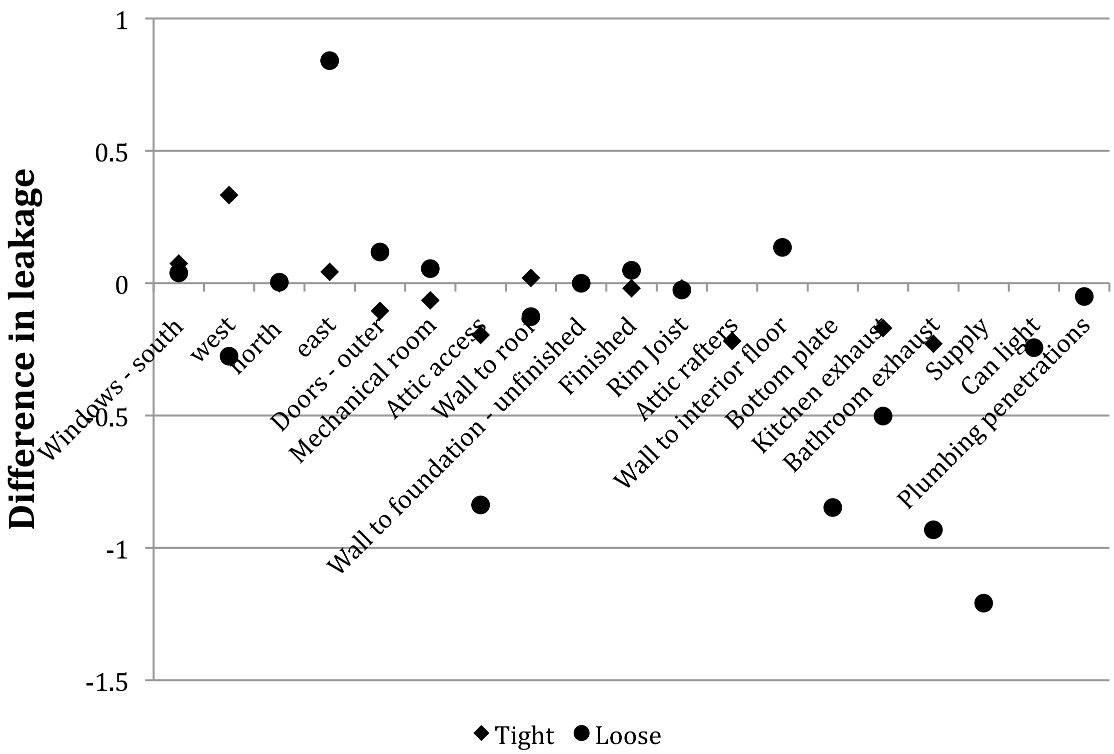

Figure 4.7. The difference in leakage of different typical leakage sites in both the tight and loose houses reveals that the largest leakage contributors in the loose house are the bottom plate, exhausts and supplies, and the recessed lighting.

Different from the previous chart, the points here become negative frequently. This is because if there is infiltration, the numerator in the second term becomes larger, and the denominator in the second term is generally smaller due to the later time of day.

This chart shows that, at times, the loose house does have leakier windows and doors. The wall to roof, wall to foundation and rim joist connections again do not contribute a large amount of air leakage. This equation does display that the bottom plate, exhaust and supply have more leakage in the loose house, as was seen when using Equation 4-1. Finally, the recessed lighting contributes a small amount to the leakage.

There is one unusual point: the east window has a very positive contribution in the loose house. The thermal images associated with this value are surprising. The sun appears to have heated the glass-to-frame connections upwards of 95 degrees before the blower door test. The window cools considerably by the time the second image is taken, during the blower door test. This makes sense given that the window is east facing. It is subject to a large amount of sun, early in the morning. This only occurs in the loose house, which is in an open field, whereas trees surround the tight house. Therefore, the air infiltrating in the first image is much warmer than in the second, making the difference in leakage very positive. However, this is not indicative of the amount of air leakage because the sun has such a large effect. The only conclusion is that there is some infiltration.

Overall, it seems that the windows and doors contribute a modest amount and the bottom plate and exhausts contribute more to the leakage. To understand this more, retrofits in the looser house are conducted, which are discussed in the next section.

4.2.3. Discussion

In general, the thermal imaging reveals that windows, doors, bottoms plates, exhausts, supplies and recessed lighting contribute to air leakage. Interestingly, the relative leakage equation and the difference in leakage equation, which at times use different air leakage locations, have similar results. This may be because the houses are genuinely leaking from all of those locations. A possible uncertainty, however, is that different materials have different conductivities. A material may not appear very cold in the first image but if the blower door caused some air leakage, the material could become cold because it is conductive. Therefore, it is difficult to determine the extent of leakage using thermal imaging (Kalamees, 2008). However, there is an indication of infiltration either way, and the location must be retrofitted to reduce energy use.

Another interesting note is the supposedly large leakage contribution of the supply ducts. It is very difficult to understand if this is air leakage, or if the difference in temperature over time is due to the fact that the HVAC system is turned off when the experiment begins. A better method of testing duct leakage – testing with the ducts open and then covered – was explored in Section 3.3.2 of this thesis.

One final problem is the effect of the sun, discussed previously. The temperature of the air that the blower door is pulling in may be larger than the outside temperature documented. To better understand the effect of the sun, taking thermal images of the outside of the house would be valuable. This may also help determine air leakage pathways.

Another critique of the process is that thermal images are not taken of the recessed lighting in the tight house. It is therefore not possible to compare their contribution.

4.3 Sequential Blower door testing

4.3.1 Methodology

Another method to understand a site's contribution to leakage is through sequential blower door testing. This involves performing a blower door test, sealing a leak, and then testing again (Armstrong et al., 1996). Because of time limitations, sometimes a full blower door test is done and sometimes a reading at 50 Pascals is taken. Taking a reading at high pressure is quite common because it ensures that the flows measured are not as affected by experimental variation (Sherman and Chan, 2004). When a full blower door test is done, temperatures both inside and outside the house and wind speeds on the west side of the house were taken.

The retrofits that are performed are in chronological order below. If a full blower door test follows a retrofit, [full] is written after the process. Otherwise, [point] is written afterwards.

1. Fix a water leak in the ceiling [full]
2. Tape plastic sheeting over a laundry chute [point]
3. Caulk around the windows [full]
4. Caulk around doors leading directly to the outside [point]
5. Caulk around doors leading indirectly outside (i.e. to the basement) [point]
6. Seal rim joists in the basement using spray foam insulation [full]
7. Seal mechanical penetrations from the basement to the first floor using spray foam insulation [point]
8. Seal bottom plates in the attic using spray foam insulation [point]
9. Cover 46/60 of the recessed lights on the first floor using plastic sheets [full]

These tests are examined by plotting all the flows versus the pressures that produce them. This way, it is easier to see whether the same pressures cause lower flows due to retrofits. The four full blower door tests are compared using the Wilcoxon signed-rank test, a non-parametric test to compare two related samples (Rice, 2007). Then, the air leakage is calculated for each full test using the process laid out in ASTM standard E779. These values are compared both as-is and after normalization. The final step is to determine how large a change the retrofits made by examining the normalized leakage of the loose house, originally and post-retrofit.

4.3.2 Results

As described above, blower door tests are run during the retrofit process. The flow versus pressure chart produced can be seen in Figure 4.8, below.

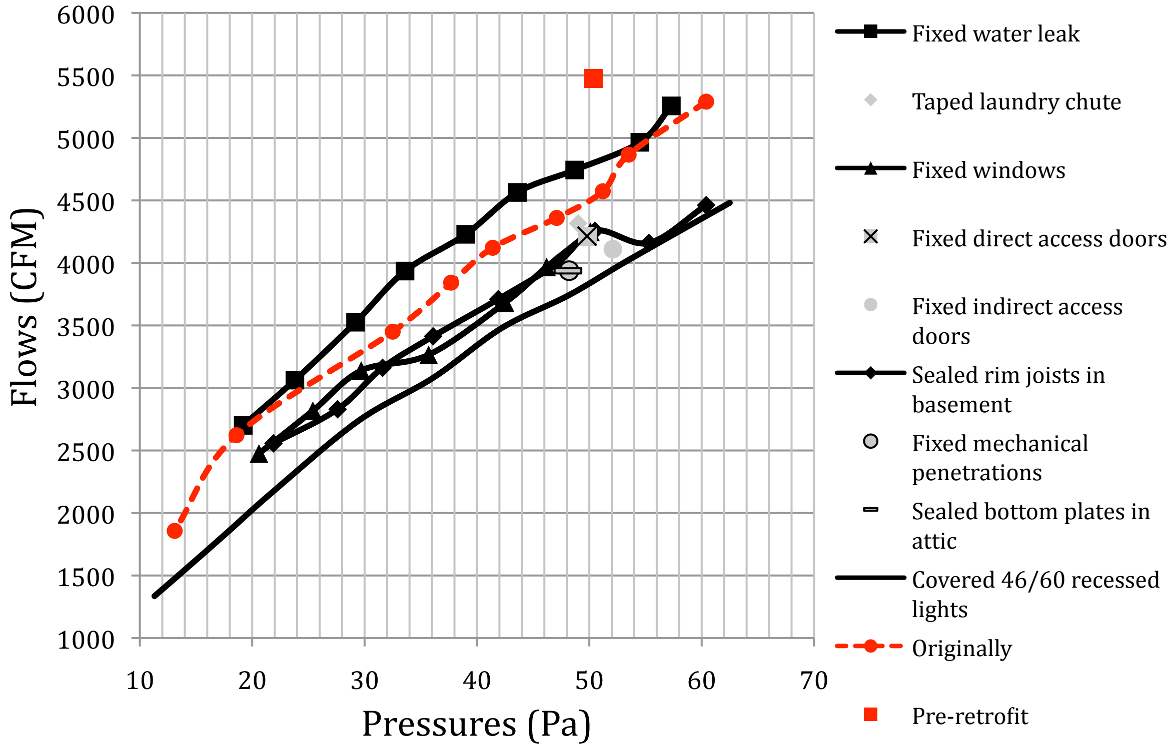

Figure 4.8. Flows versus pressures during sequential blower door testing in the loose house display that the laundry chute and the recessed lighting cause the largest decrease in flows.

The "original" line is the test taken about one year ago when this research began. In the interim, a water leak caused a hole in the ceiling, explaining the high flow rate for the "pre-retrofit" point. The water leak is fixed, and the flow rate results decrease to values similar to the original test. In the analysis, these results are considered equivalent.

The next retrofit involves covering the laundry chute with plastic. Interestingly, the laundry chute passes through the rafters without any sort of barrier. This can be seen in Figure 4.9. This is covered so that air is not moving into the rafters, and the flow rate at 50 Pascals decreases. The tests that follow do not change the flow rate significantly, including caulking around the trim of the windows and doors, sealing the rim joists and mechanical penetrations and sealing the bottom plates using spray foam insulation. Pictures of the retrofitting process can be seen in Figure 4.10.

Figure 4.9. The laundry chute goes through the rafters without a barrier.

Figure 4.10. Sealing the rim joists and the plumbing penetrations in the loose house did not greatly affect the flow rates during the blower door test.

Finally, 46 out of 60 of the recessed lights on the first floor are covered with plastic. This causes a large decrease in flow rate during the blower door test.

The next step in this process is to determine how big a change the retrofits make. In Figure 4.11, the normalized leakage of the loose house originally, the loose house post-retrofit and the tight house can be seen, plotted over a graph shown earlier in this thesis, comparing ICF to wood home data. Overall, the house decreases in air leakage, in units of cm^2, by 30%. Clearly, although the retrofits help, they are not enough to decrease the air leakage even to the median found among the ICF houses.

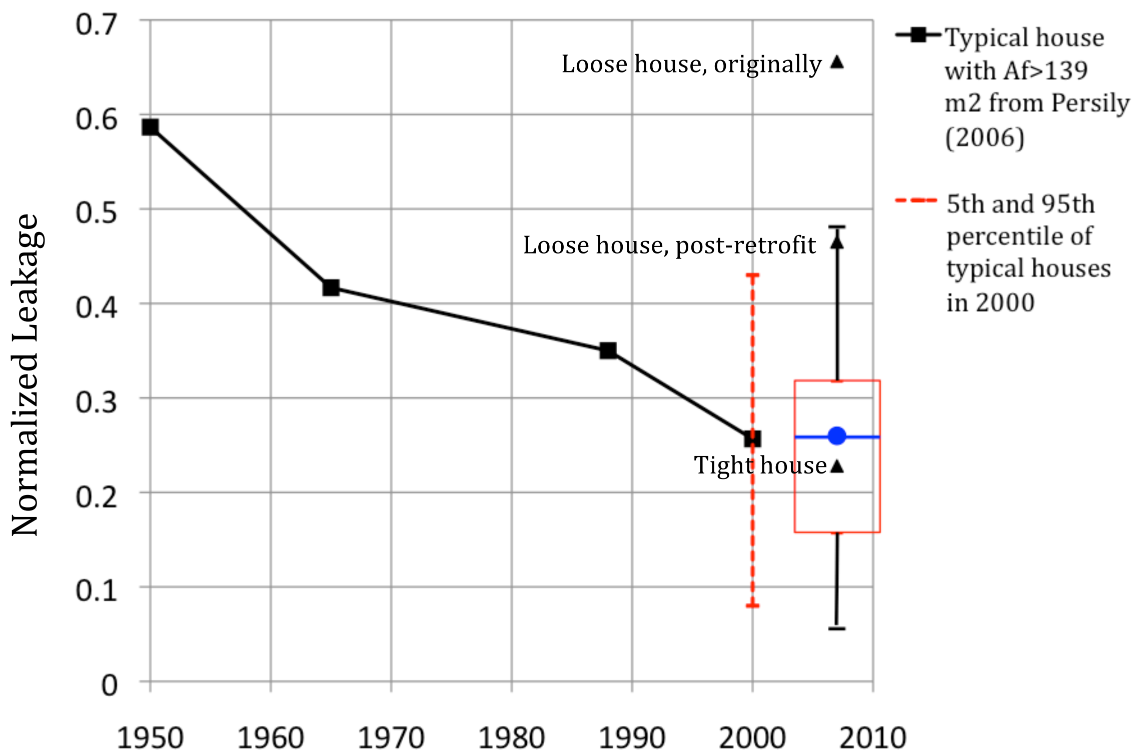

Figure 4.11. The chart comparing ICF and wood houses, with the loose house both pre and post retrofit and the tight house overlaid at values of 0.656, 0.465, and 0.228, respectively. The retrofits did help reduce the air leakage of the loose house by 30%, but not enough to reach the median of the ICF data.

4.3.3 Discussion

The only instance in which a significant difference between the blower door tests is achieved is when the original line and the data after covering the lights, the last test, are compared. This significant difference is achieved through two specific retrofits: covering the laundry chute and the lights.

The single recorded point for the laundry chute at approximately 50 Pascals is on the same general line as the windows. Covering the laundry chute produces the decrease between the original line and the line generated after fixing the windows. Covering the lights causes the other decrease in flows. Therefore, it is clear that covering the laundry chute and the lights creates the significant change in air leakage observed. The other tests all generally fall on the same line.

The fact that windows, doors and bottom plates are not found to be important during sequential blower door testing is contrary to what is observed during thermal imaging, where they added a modest amount of leakage. This could be because, although the windows, doors, and bottom plates are sources of air leakage, the caulk and spray-foam insulation do not significantly alter the flow. In addition, the window and stud wall may leak in locations that are not retrofitted. This is very likely based on the thermal imaging results. Finally, it may be due to the fact that the blower door is not sensitive to small changes.

Another source of uncertainty in this test is the wind speed and direction. Although measured, it is quite variable and difficult to document.

In terms of the process, it would have been useful to cover the fireplace with plastic and understand its contribution to air leakage. However, it is a gas, ventless fireplace and therefore probably not a large source of leakage, as opposed to wood fireplaces. In addition, the most minor changes to the house should have been made last to reduce uncertainty attributed to the sensitivity of the blower door.

Although 30% of the air leakage is accounted for, there is still a large difference between the loose and tight house. There are many possible explanations for this. First, there is a difference in the number of recorded leakage sites. The loose house has 26 windows, with a total of 0.23 square meters (357 square inches) of window area, while the tight house has 22 windows and 0.18 square meters (286 square inches). Therefore, if the windows leak, the loose house should have a higher leakage area because it has more windows. The number and area of the doors are similar. The ratio of volume and surface area of the loose to tight house is 1.6 and 2.0, respectively. This is a large difference, and almost certainly has an effect when considering air leakage through the bottom plate, for example. Thirdly, as noted previously, although certain locations are retrofitted, they leak in other locations as well, based on the thermal imaging. For example, the window and door trim was caulked where it meets the wall but there is also leakage at the window-frame interface. In addition, the top plates, which connect the studs to the overall house, may leak like the bottom plates.

Another possible reason for the difference in air leakage between the loose house and the tight house is the ducts. These were tested, as described in the previous chapter, and the results for the loose house show that there is less leakage when the ducts are open. Obviously, this is very surprising and shows that more investigation is necessary to understand their contribution.

Finally, the bathrooms in the loose house are vented directly to the soffits. This corroborates well with the thermal imaging results that display the large contribution of exhaust ducts to air leakage. Because these are not retrofitted or covered temporarily, they are contributing to the difference.

4.4. Consolidated Findings and Verification

Based on the tests done in Nashville, several conclusions can be drawn. First, windows and doors do contribute to infiltration. Although retrofits were completed unsuccessfully, they were not in all of the important locations, namely where the glass meets the casing and where the casing meets the trim. The former probably depends on the window and door manufacturer more than the construction. Therefore, it is still important to give glazing and door leakage consideration.

The other large contributors to air leakage discussed are the bottom plates, exhaust vents, supply vents, and recessed lighting. Given that the supply vents were turned off at the beginning of the test and that their change in temperature may have been due to natural cooling rather than leakage, it is difficult to reach a conclusion about them. The other three sources have attic leakage as a shared attribute, as can be seen in Figure 4.12. The bottom plate causes leakage from the upstairs conditioned rooms to the attic, and the recessed lights and exhaust fans are installed directly into the attic floor. Because the attic space has open ridge and soffit vents, air can easily escape from the house.

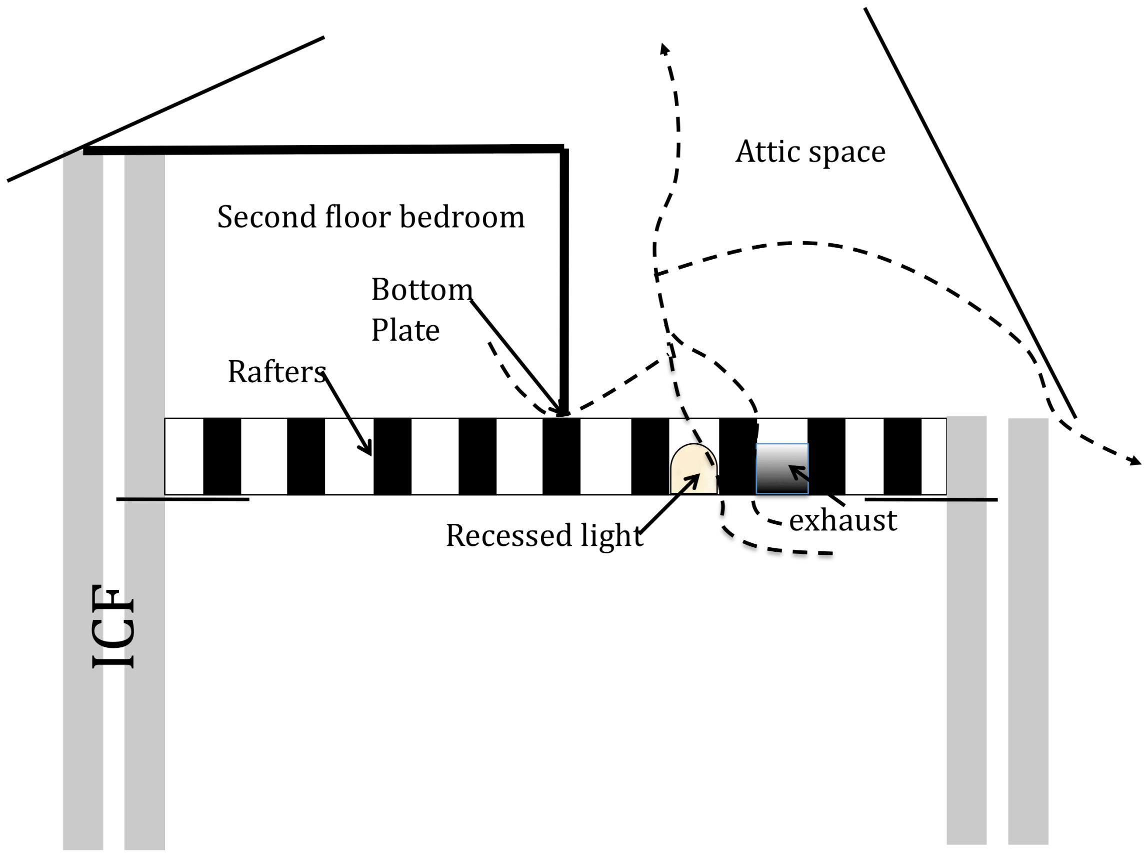

Figure 4.12. Diagram of the infiltration pathways to the attic that are a large source of air leakage in the loose house including the bottom plate, recessed lights, and exhaust vents.

In the tight house, the attic can be described as a conditioned space; it is insulated and has an air barrier on the rafters. In the loose house, there is insulation in the decking but no air barrier. If there is an air barrier in the rafters, which was not verified, it is not useful because the soffit and ridge vents are completely open. This could be one of the characteristics causing the large difference between the tight and loose house.

In order to have confidence in the thermal imaging and sequential blower door testing described in this chapter, the results are compared to another source. ASHRAE Fundamentals compiles many different studies' results on the contribution of different aspects of building elements to air leakage (ASHRAE Fundamentals, 2009). A summary is:

- Walls: 35%
  - This includes cracks between components such as top plates, outlets, and plumbing penetrations
- Ceiling details: 18%
  - Including recessed lighting
- HVAC systems: 18%
- Fireplaces: 12%
- Vents: 5%
- Diffusion through walls: <1%

Qualitatively, these results are similar to the results found in this thesis, namely that windows, doors, bottom plates, exhausts/supplies and recessed lighting are the biggest contributors to the air leakage.

4.5. Recommendations

There are many organizations that recommend certain measures for air sealing. Energy Star describes obvious locations – windows and doors – and others such as attics and basements, as important sites to seal. They recommend using caulk, spray-foam or weather stripping (US EPA, 2012).

The Passivhaus standard, which requires very low levels of air infiltration, has more rigorous recommendations. They advise creating an airtight barrier using a parging coat, a membrane or timber sheets. In addition, if there is an interruption in this barrier such as a window, Passivehaus recommends the use of propriety tape (Building Research Establishment, 2012).

The Department of Energy published an air-sealing guide in 2010 that goes into much more detail. This includes a list of 19 typical leakage locations, including:

1. Air Barrier and Thermal Barrier Alignment
2. Attic Air Sealing
3. Attic Kneewalls
4. Shaft for Piping or Ducts
5. Dropped Ceiling/Soffit
6. Staircase Framing at Exterior Wall
7. Porch Roof
8. Flue or Chimney Shaft
9. Attic Access
10. Recessed Lighting
11. Ducts
12. Whole-House Fan
13. Exterior Wall Penetrations
14. Fireplace Wall
15. Garage/Living Space Walls
16. Cantilevered Floor
17. Rim Joists, Sill Plate, Foundation, Floor
18. Windows & Doors
19. Common Walls Between Attached Dwelling Units

The guide also explains how to prevent air leakage in general and during the retrofit process (US DOE, 2010).

Based on the tests done in Nashville, there are several recommendations that can be made to reduce air leakage. These are similar to those described above, but have been pared down to what was found to be the most important for ICF houses.

First, the windows and doors are judged to be leaky in locations assembled during manufacturing, based on the thermal images. For example, it was typically colder where the window glass meets the wood frame. Therefore, it is important to go back to the manufacturers and determine the most airtight design for operable windows.

The attic is also considered a major source of air leakage due to bottom plates, exhaust vents, and recessed lighting. A solution to this problem is a true air barrier in the loose house. Because moisture can be a problem in attics, an air barrier on the decking would be logical. However, if there is some controlled ventilation and the bathroom exhausts are not connected to the attic, but rather feed air directly outside, it is possible to have an air barrier on the rafters, as was done in the tight house. Either method would greatly reduce the air leakage in the loose house, and could contribute to bringing the air leakage values down to the median found for ICF houses.

4.6. Conclusions

This chapter:

1. Describes the process of thermal imaging and sequential blower door testing on a looser and tighter house in Nashville, TN, as well as the results from these tests.
2. Displays that cracks around windows and doors cause some air leakage. However, the locations where they have cracks are variable and different steps are necessary to ensure that they are tight.
3. Proves that attic leakage due to elements such as bottom plates, exhaust, laundry chutes and recessed lighting contribute to the large difference between the loose and tight houses in Nashville.
4. Recommends more tightly sealed windows and doors, and that either attics be considered unconditioned spaces and an air barrier be installed over the decking or that they be considered conditioned and the insulation and air barrier be installed in the rafters.

The next question to address is how the range in air leakage affects the energy use of houses. This is discussed in the next chapter of this thesis.

5. Energy Use of Single Family Houses

5.1 Introduction

As seen in chapter 4 of this thesis, there is a large range in leakage area of ICF houses. However, the effect this range has on energy use is unknown. In order to understand the importance of these values and their variability, Amanda Webb collaborated on this project to create an energy model using EnergyPlus (EnergyPlus, 2010). EnergyPlus is a building energy simulation program that bases its calculations on the integration of building loads and building response. The loads on the building are calculated and fed back, iteratively, to the building's response. For example, if the loads on the building determine that the zone requires heating, the heating system will be turned on and the loads will be calculated again. Besides information about the building, such as internal loads and construction materials, a TMY3 weather file is input for the building's location in order to specify the most likely weather loads on the building.

The purpose of this chapter is to first create a model of a typical single-family house, with a very clear understanding of its infiltration calculation. Using this model, the next step is to input different values of infiltration based on the comparison between wood-stud and ICF in Chapter 3. By running the energy simulation after only changing this variable, the effect of different values of infiltration can be clearly displayed.

This chapter details:

1. The creation of this energy model, including the inputs related to the geometry, construction, internal loads and HVAC system.
2. The set of formulas which use values from Chapter 3, the weather file, and characteristics of the typical single-family house to calculate air leakage.
3. Trends in energy use calculated by the energy model.

5.2 Creating the model

5.2.1 The guidelines

Ms. Webb used the Building America House Simulation Protocol 2010 (BAHSP, 2010) to create an EnergyPlus model of a typical single-family house that meets the 2009 International Energy Conservation Code (IECC). The US Department of Energy's National Renewable Laboratory created this document. Similar to ASHRAE's Standard 90.1 Appendix G, which addresses typical commercial buildings, it provides a modeling methodology for a typical house in the United States. For more detail, see the report by Ochsendorf et al. (2011).

5.2.2 Properties of the model

First, the single-family house is modeled in two locations: Chicago and Phoenix. This provides an understanding of the energy use of the house in both a heating-dominated and cooling-dominated climate.

Based on the BAHSP model, the house is 222 square meters (2,400 square feet) and has 15% glazing. It has two floors and an unconditioned attic. This is modeled with three zones: one conditioned, one plenum and one unconditioned zone. The aspect ratio is 1:1.2. The roof, partitions and floors are the same in both houses, and summarized in Table 5-1. These were designed based on consultations with local builders.

Table 5-1. Similar properties of the single-family house.

Roof	
Pitch	6:12
Shingles	Asphalt
Sheathing	½ in (12.7 mm) Plywood
Insulation	Fiberglass-batt
Drywall	½ in (12.7 mm) thick
Rafters	2x10 (38 mm x 235 mm) @ 16 in (406 mm)
Load Bearing Partitions	
Studs	2x4 (38 mm x 89 mm) @ 16 in (406 mm) O.C.
Drywall	½ in (12.7 mm) thick
Floors	
Sheathing	5/8 in (15.9 mm) Plywood Sheathing
Joists	9-½ in (241 mm) I-Joists @ 16 in (406 mm)
Drywall	½ in (12.7 mm)

The internal loads include 2.64 people and typical lighting and equipment for the year. These values can be seen in Table 5-2.

Table 5-2. Equipment loads in the single-family house.

Lighting	Btu/ft^2 (W/m^2) 1.04 (3.29)
Equipment	Btu (W)
Refrigerator	311 (91.1)
Cooking Range	701 (206)
Clothes Washer	74.4 (21.8)
Clothes Dryer	977 (286)
Dishwasher	198 (58.1)
Misc Electric load	1950 (571)
Misc Gas Load	38.6 (132)

The HVAC system is an air loop with a gas burner, cooling coil, and dehumidifier. There is also a whole house exhaust fan to meet ASHRAE 62.2 standards (2003). More details on this system can be seen in Table 5-3.

Table 5-3. Values associated with the HVAC system in the single-family house.

Input	Value
Supply airflow rate	Determined by EnergyPlus
Fan efficiency	0.389
Gas burner efficiency	0.805
COP of cooling coil	3.895
Energy factor of dehumidifier	1.1
Water heater efficiency	0.78

Outside air is only provided by infiltration. Natural ventilation is employed on specific days if certain conditions are met, including the ability to maintain indoor temperatures and the relative humidity of the outdoor air.

The properties of the windows in the model are given in Table 5-4. They are double-paned and insulated.

Table 5-4. Properties of the windows in the single-family house model.

	U value Btu/hr-ft^2-F (W/m^{2}K)	Solar Heat Gain Coefficient
Chicago	0.35 (1.99)	0.35
Phoenix	0.40 (2.27)	0.30

Two types of wall constructions are modeled in the house: wood-stud and insulated concrete form. The wood-stud wall is a series of four materials: exterior finish, 5/8" plywood, stud and cavity layer, and gypsum board. The properties of the stud and cavity layer are based on a surface area weighted-average of the different materials' properties.

The ICF is 6" of concrete with 2.5" of insulation on either side, and is modeled as such. It also has an exterior finish and gypsum board, similar to the stud wall. A summary of the construction can be seen in Table 5-5. Both of these structures were checked with the requirements of local building codes.

Table 5-5. Details of the two types of wall construction.

	ICF – Chicago	ICF – Phoenix	Wood – Chicago	Wood - Phoenix
Exterior Walls				
ICF Wall	6 in (15.2 cm) core	6 in (15.2 cm) core	N/A	N/A
EPS Insulation	2.5 in (63.4 mm) panels	2.5 in (63.4 mm)	N/A	N/A
Studs	N/A	N/A	2x6 @ 24 in o.c. (38 mm x 140 mm @ 61 cm o.c.)	2x4 @ 16 in o.c. (38 mm x 89 mm @ 41 cm o.c.)
Sheathing	N/A	N/A	5/8 in (15.9 mm) Plywood	1/2 in (12.7 mm) Plywood
Insulation	N/A	N/A	Fiberglass	Fiberglass
Drywall	½ in (12.7 mm)	½ in (12.7 mm)	½ in (12.7 mm)	½ in (12.7 mm)

The resulting R-values and thermal mass in these walls can be seen in Table 5-6.

Table 5-6. Thermal resistance requirements and values, and thermal mass values of the single-family house are the same for all building elements except the exterior walls where ICF has both a greater R-value and a greater thermal mass.

		R values ft²·°F·h/Btu (m²K/W)			Thermal mass Btu/ft²°F (kJ/Km²)	
		Wood Frame Requirements	Wood	ICF	Wood	ICF
Exterior Wall	Chicago	20 (3.52)	17.1 (3.01)	21.9 (3.86)	2.4 (48.5)	14.2 (290)
	Phoenix	13 (2.29)	10.6 (1.87)		2 (41.8)	
Ground Floor	Chicago	10 (1.76) for 24 in (61 cm)	13.6 (2.40)		15.7 (323)	
	Phoenix	0	9.6 (1.69)			
Attic Floor	Chicago	38 (6.69)	37.7 (6.64)		0.52 (10.6)	
	Phoenix	30 (5.28)	29.7 (5.23)		0.49 (10.0)	

The ICF exterior wall has a larger R-value and thermal mass, due to its concrete, compared to the wood construction. All other values are constant between the two. Its larger R-value will enable the wall to resist movement of heat both into and out of the house, saving energy. In addition, by dampening temperature swings that the house is subject to, the thermal mass also lowers the energy use of the ICF house in the model.

5.3 Infiltration in the model

There are many ways to enter values of infiltration in EnergyPlus. The one chosen for this research is based on the enhanced model put forth by ASHRAE 2009 Fundamentals. These equations, which are based on inputs about the house, the indoor-outdoor temperature difference, Δt, and the wind speed, U, are presented in Equations 5-1 through 5-4. First, the volume flow rates are calculated. Q_s, the stack flow rate, is due to buoyancy flow, or a difference in temperature. Q_w, the wind flow rate, is the amount of air infiltration due to wind pressures. These ambient conditions are taken from the weather file. The coefficients in Equations 5-1 and 5-2 are based on experimental data and properties of the house. Then, the volume flows are summed in quadrature to create a total flow rate due to infiltration, as seen in Equation 5-3. This value is combined in quadrature with other types of unbalanced ventilation, such as bathroom exhaust, and added to the amount of balanced ventilation for the total flow rate in Equation 5-4. The total is input into the Zone Infiltration object in EnergyPlus.

$$Q_s = cC_s\Delta t^n$$

$$Q_w = cC_w(sU)^{2n} \quad (5\text{-}2)$$

$$Q_{infiltration} = \sqrt{Q_s^2 + Q_w^2} \quad (5\text{-}3)$$

$$Q_{combined} = Q_{balanced} + \sqrt{Q_{unbal}^2 + Q_{infiltration}^2} \quad (5\text{-}4)$$

where
c, n = coefficient and exponent which specify the air leakage in a house, $m^3/(s/Pa^n)$ and dimensionless, respectively
s = the shelter factor, dimensionless
C_s, C_w = stack and wind effect coefficients, $(Pa/K)^n$ and $(Pa*s^2/m^2)^n$, respectively
Δt, U = Difference in temperature and the wind speed, based on the weather file, ˚C and m/s, respectively
Q_s, Q_w = volume flow rates, m^3/s

To change the amount of infiltration, either the *c* or *n* values can be varied. Because the comparison between wood and ICF houses is done using normalized leakage values, as seen in the third chapter of this thesis, this is the starting point for determining the c and n values. First, normalized leakage is used to calculate leakage area, based on the defining formula, Equation 5-5, and the properties of the house being modeled:

$$NL = 1000 * \frac{A_L}{FloorArea}\left(\frac{Height}{2.5}\right)^{0.3} \quad (5\text{-}5)$$

where
Floor area of modeled home = 222 m^2 (2400 ft^2)
Height of modeled home = 4.88 m (16 ft)
A_L = leakage area, m^2

Based on A_L, the flow rate Q can be calculated using Equation 5-6, which is derived from the Bernoulli equation.

$$Q = A_L\sqrt{\frac{2 * P_r}{\rho}} \quad (5\text{-}6)$$

where
P_r = the reference pressure, 4 Pascals
ρ = the density of air, 1.2 kg/m^3
Q = the volume flow rate, m^3/s

Finally, Q is a function of both *c* and *n*, as seen in Equation 5-7. Because *n* is typically considered to be 0.65, *c* can be calculated and input into EnergyPlus (ASHRAE, 2009).

$$Q = c\Delta P^{n} \qquad (5\text{-}7)$$

where
n = the pressure exponent, dimensionless
c = the flow coefficient, $m^3/s/Pa$

Table 5-7 contains values of normalized leakage for the different house types and the c values that are calculated using these numbers.

Table 5-7. Values of NL and c for the loose, average, and tight ICF and wood houses. The *c* values were used as input into the model of a single-family house in EnergyPlus.

	Normalized Leakage	
	ICF	Wood
Maximum	0.4811	0.4300
Median	0.2599	0.2567
Minimum	0.0557	0.0800
	c Values	
Maximum	0.0916	0.0819
Median	0.0495	0.0489
Minimum	0.0106	0.0152

The c values are input into EnergyPlus for both Chicago and Phoenix. Therefore, a total of 12 models are run.

5.4 The results

The chart in Figure 5.1 displays the energy consumption of a single-family house in Chicago. For the ICF house, the energy use is 184, 155, and 135 $kWh/m^2/year$ for the loose, median, and tight air leakage, respectively. For the wood-stud house, these values are 185, 162 and 144 $kWh/m^2/year$. These numbers do not vary due to changes in equipment, lighting or Domestic Hot Water (DHW) energy use, which remain constant because wall construction and air tightness do not affect them. Only energy related to the HVAC system including fans and pumps, cooling, and heating cause the variation in consumption. The reason the ICF house uses consistently less energy than the wood-stud house is a combination of its larger R-value and thermal mass.

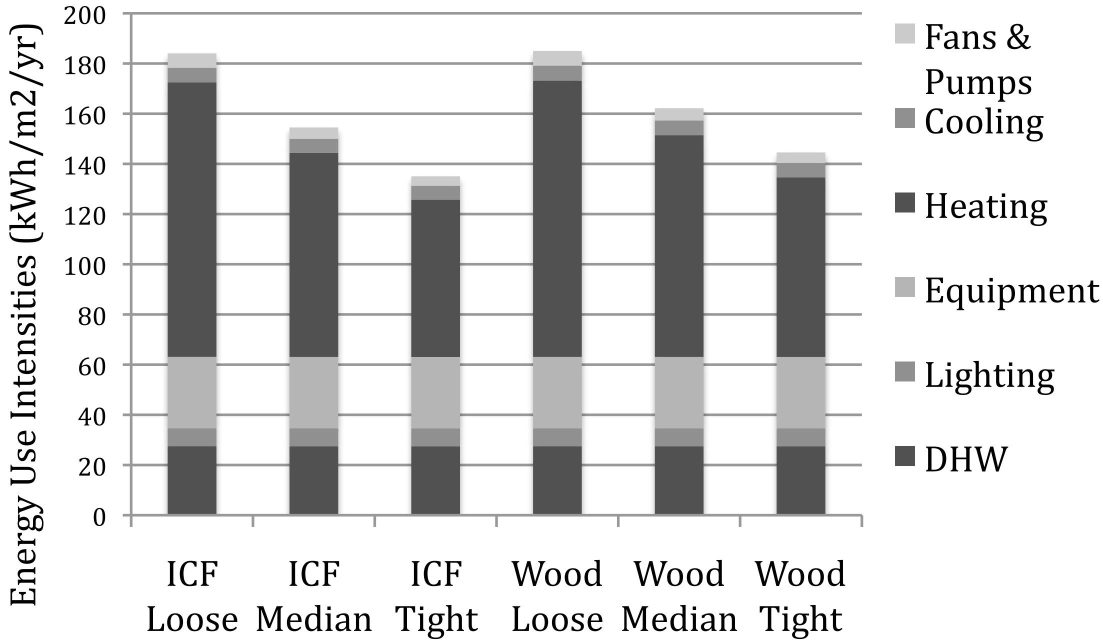

Figure 5.1. The energy use (kWh/m^2/year) in Chicago for the ICF and wood wall constructions at three different levels of air tightness. The difference between the wall constructions is small compared to the difference due to variable leakage area.

The chart in Figure 5.2 displays the energy consumption in Phoenix. For the ICF house, the energy use is 86, 83, and 78 kWh/m^2/year for the loose, median, and tight air leakage, respectively. For the wood-stud house, these values are 94, 91 and 85 kWh/m^2/year. Again, the ICF house consumes less energy because its exterior walls have a higher R-value and contain more thermal mass.

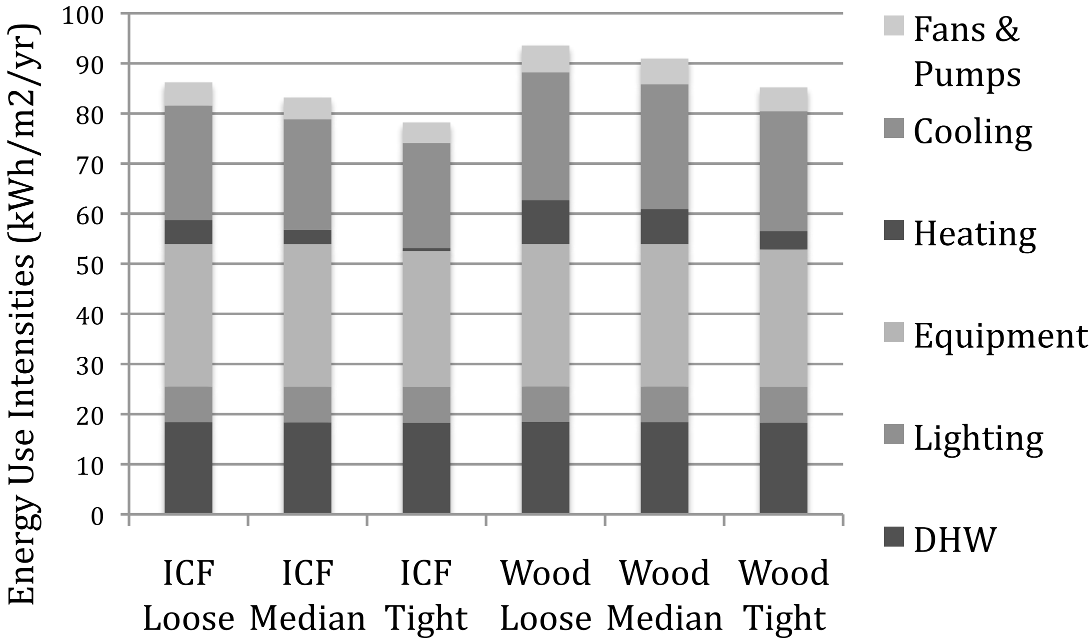

Figure 5.2. The energy use (kWh/m^2/year) in Phoenix for the ICF and wood wall constructions at three different levels of air tightness. The difference between the wall constructions is small compared to the difference due to variable leakage area.

5.5 Discussion

5.5.1 The wall construction

The first conclusion that can be drawn from the graphs in Figure 5.1 and Figure 5.2 is that the amount of infiltration greatly affects the energy use. In Chicago, tightening a house from loose to tight, no matter which construction method is used, can decrease the energy consumption by an average of 24%. In Phoenix, there is a mean savings of 9%. The reason for this difference is climate. Although Phoenix has a very hot climate, Chicago is much colder. The sum of the difference over the course of a typical year between the outdoor temperature and a comfortable body temperature, taken to be 25 degrees Celsius, is larger in Chicago than Phoenix. In other words, Chicago temperatures differ more from comfort conditions than Phoenix weather, overall. Therefore, air leakage plays a more important role. Chicago houses use 46% more energy than those in Phoenix, on average.

It is also clear that the same air leakage with a different wall construction has very similar energy use. Interestingly, when comparing different wall constructions with the same airtightness, Chicago wood and ICF energy use is more similar than wood and ICF in Phoenix. The variation between wood and ICF is 6 kWh/m^2/year in Chicago and 7 kWh/m^2/year in Phoenix for the median leakage. The difference in building code is the cause of this. The building code for a wood-stud house in Phoenix is more lax in its insulation requirements than Chicago, but a mass wall remains constant in both climates. Therefore, the difference between wood and ICF construction is greater in Phoenix, and a greater difference in energy use can be seen.

In addition, it is important to note that the variation between wood and ICF discussed above is not solely due to airtightness, although there is a difference in c values as can be seen in Table 5-7. ICF also has a greater R-value and amount of thermal mass than wood.

In order to understand the contribution of infiltration versus insulation and thermal mass, the amount of infiltration is held constant in Chicago. The infiltration of the wood house is applied to the ICF house– from c = 0.0495 to c = 0.0489. Therefore, the energy use of the ICF house decreases. The difference between the ICF and wood houses is originally 7.67 $kWh/m^2/year$, with ICF using less energy. Because the ICF house now consumes an even smaller amount of energy, the difference increases to 8.07 $kWh/m^2/year$. The change in the difference in energy use is 0.4 $kWh/m^2/year$ and shows that infiltration has a much smaller effect on the energy use than the R-value and thermal mass when comparing median air leakage.

5.6 Conclusions

This chapter:

1. Creates a model in EnergyPlus of a typical single-family house in the United States with a clear set of rules for defining infiltration.
2. Shows that the amount of infiltration greatly affects the energy use – the difference between a loose and tight house in Chicago is 24% and in Phoenix it is 9%.
3. Displays the importance of climate. Chicago houses use 46% more energy than those in Phoenix, on average, because of the harsher Chicago temperatures.
4. Proves that the difference in energy use between wood and ICF houses with the same level of air leakage is negligible.

6. Conclusions

This thesis first examines research previously done on air leakage, insulated concrete form, and how these variables affect energy use. There is currently no study that compares the air leakage of a collection of ICF and wood-stud construction single-family houses. In addition, no study uses information on leakage sites to understand variability among houses with different types of envelopes. Finally, building energy simulations of a typical US house with justifiable values of air leakage are rare. There are clearly large gaps in our understanding of air leakage, which are addressed in this thesis.

In Chapter 3, a collection of 43 blower door tests of ICF houses is assembled. These tests are analyzed and it is determined that, although the leakage area values tend towards smaller numbers, the range is still quite large. A possible cause of this large variation is differences in volume and window area, which are established as the best predictors of leakage area. Finally, the normalized leakage of ICF and wood houses are compared and found to be 1.2% different.

To more closely investigate the reasons for variation among the ICF blower door tests, Chapter 4 reports on the examination of a very leaky ICF house and a tight ICF house from the data set. Based on thermal imaging and sequential blower door testing, it is determined that cracks around windows and doors cause some air leakage, and that attic leakage due to elements such as bottom plates, exhaust, laundry chutes and recessed lighting cause a large amount of air leakage. Therefore, the detailing of the joints can greatly effect how much air is flowing in and out of a house. However, the leakage in the loose house is diminished by 30% through retrofits in the course of one day.

In order to understand how changes in air leakage affect energy use in houses, a colleague created an energy simulation of a typical US house based on the Building America House Simulation Protocol. By comparing three levels of air leakage of ICF and wood-stud construction in Chicago and Phoenix, it is clear that the level of infiltration and the climate greatly affects the energy use.

There are several next steps to consider in this field of research. First, increasing understanding of the building stock, specifically the data in Chan (2005), may increase our knowledge of ICF houses. For example, dividing the data by construction type instead of assuming it is all wood frame could provide greater insight into the comparison between wood and ICF houses. In addition, testing the improvements suggested in this thesis for ICF houses is necessary for future application. This may involve retrofits or new construction but must focus on how air moves between the attic and living space. Incorporating these findings into energy models to predict future savings will also be relevant and useful.

References

Al--Homoud, M. Performance Characteristics and Practical Applications of Common Thermal Insulation Materials. Building and Environment. 40: 353 – 366. 2004.

Armstrong, P., Dirks, J., Klevgard, Matrosov, Y., Olkinuora, J., Saum, D. Infiltration and Ventilation in Russian Multi-Family Buildings. ACEEE Summer Study on Energy Efficiency in Buildings. 1996.

ARXX ICF. <http://www.arxx.com/>. Accessed March 2012.

ASHRAE Handbook of Fundamentals. Owen, M.S., Editor. American Society of Heating, Refrigerating and Air conditioning Engineers. Atlanta, Georgia. 2009.

ASHRAE Standard 62.2. Ventilation and Acceptable Indoor Air Quality in Low-Rise Residential Buildings. American Society of Heating, Refrigerating and Air conditioning Engineers. 2003.

ASHRAE Standard 119. Air Leakage Performance for Detached Single-Family Residential Buildings. American Society of Heating, Refrigerating and Air conditioning Engineers, 1988. Reaffirmed 2004.

ASTM Standard E779-03. Standard Test Method for Determining Air Leakage Rate by Fan Pressurization. ASTM Book of Standards. American Society for Testing and Materials, 2003.

Balaras, C.A., Droutsa, A.A., Argiriou, D.N., and Asimakopoulos, D.N. Potential for Energy Conservation in Apartment Buildings. Energy and Buildings. 31: 143–154. 1999.

Bassett, M.R. Building Site Measurements for Predicting Air Infiltration Rates. Measured Air Leakage of Buildings, ASTM STP 904, H.R. Trechsel and P.L. Lagus, Eds., American Society for Testing and Materials, Philadelphia, 1986: 365--383.

Becker, R. Air permeability and thermal performance of concrete block wall specimens. Journal of Building Physics. 34: 163. 2010.

Briggs, R.S., Lucas, R.G., and Taylor, T. Climate Classification for Building Energy Codes and Standards. ASHRAE Winter Meeting, Chicago, IL. January, 2003.

Building America House Simulation Protocol. Hendron, R. and Engebrecht, C. National Renewable Energy Laboratory. September 2010. apps1.eere.energy.gov/buildings/.../building_america/house_simulation.pdf

Building Research Establishment. Passivehaus Primer: Designer's Guide. <http://www.passivhaus.org.uk/filelibrary/Primers/KN4430_Passivhaus_Designers_Guide_WEB.pdf> Accessed February 2012.

Chan, W.R., Nazaroff, W.W., Price, P.N., Sohn, M.D., Gadgil, A.J. Analyzing a Database of Residential Air Leakage in the United States. Atmospheric Environment. 39: 3445-3455. 2005.

Chan, W.R., Price, P.N., Sohn, M.D., Gadgil, A.J. Analysis of U.S. Residential Air Leakage Database. LBNL Report Number 53367. 2003.

Concrete-Home.com. Copyright 2006. < http://www.concrete-home.com> Accessed March 2012.

Doebber, I.R. Investigation of Concrete Wall Systems for Reducing Heating and Cooling Requirements in Single Family Residences. Master's Thesis. Virginia Polytechnic Institute. 2004.

Dickerhoff, D.J., Grimsrud, D.T., Lipschutz, R.D. Component Leakage Testing in Residential Buildings. Presented at the 1982 Summer Study in Energy Efficient Buildings. California. 1982.

Electro Optical Industries Inc. Material Emissivity Properties. <http://snap.fnal.gov/crshield/crs-mech//emissivity-eoi.html> Accessed February 2012.

Emmerich, S.J. and Persily, A.K. Energy Impacts of Infiltration and Ventilation in US Office Buildings Using Multizone Airflow Simulation. Proceedings of ASHRAE IAQ and Energy Conference. Louisiana: 191-203. 1998.

Emmerich S.J., Dowell, T., and Anis, W. Investigation of the Impact of Commercial Building Envelope Airtightness on HVAC Energy Use. National Institute of Standards and Technology. 2005.

Engineering Toolbox. Emissivity Coefficients of Some Common Materials. <http://www.engineeringtoolbox.com/emissivity-coefficients-d_447.html> Accessed February 2012.

EPA. Energy Consumption by Sector, 1949-2009. <http://www.eia.doe.gov/emeu/aer/pdf/pages/sec2_6.pdf>

EPA. Major Fuel Consumption by End-Use for All Buildings. 2003. <http://www.eia.doe.gov/emeu/cbecs/cbecs2003/detailed_tables_2003/2003set19/2003pdf/e01a.pdf>

Fluke Corporation. Founded 1948. <www.fluke.com>

Fluke SmartView Thermal Imaging Analysis and Reporting Software. Version 3.1. Plymouth, MN. 2009.

Frye, A. Energy Efficiency's Role in a Zero Energy Building: Simulating Energy Efficient Upgrades in a Residential Test Home to Reduce Energy Consumption. Masters Thesis. University of Tennessee at Chattanooga. 2011.

Gammage, R.B., Hawthorne, A.R., White, D.A. Parameters affecting air infiltration and airtightness in thirty--one East Tennessee Homes. Measured Air Leakage of Buildings. ASTM STP 904. H.R. Trechsel and P.L. Lagus, Eds., American Society for Testing and Materials, Philadelphia: 61-69. 1986.

Gettings, M.B., McCold, L.N., Schlegel, J.A. Field Test Evaluation of Conservation Retrofits of Low-- Income, Single-Family Buildings in Wisconsin: Blower-Door Directed Infiltration Reduction Procedure, Field Test Implementation and Results. ORNL Con--228 P5. 1988.

Infrared Services Inc. Emissivity Values for Common Materials. <http://infrared-thermography.com//material-1.htm> Accessed February 2012.

ICF Facts. <www.ICFhomes.com>. Accessed March 2012.

Insulated Concrete Form Association. Established 1995. < http://www.forms.org>

Kalamees, T., Korpi, M., Eskola, L., Kurnitski, J., Vinha, J. The distribution of the air leakage places and thermal bridges in Finnish detached houses and apartment buildings. Proceedings of the 8th symposium on Building Physics in Nordic Countries. Copenhagen, Denmark. 2008.

Kosny, J., Christian, J.E., Desjarlais A.O., Performance Check between Whole Building Thermal Performance Criteria and Exterior Wall Measured Clear Wall R-Value, Thermal Bridging, Thermal Mass, and Airtightness. *ASHRAE Transactions.* 104 (2): 1379-1389. 1998.

Lawrence Berkeley National Laboratory. Residential Building Systems. <http://homes.lbl.gov/>

Matlab. Version 2011a. The MathWorks Inc. Natick, Massachusetts: 2011.

Nabinger, S., Persily, A.K., Impacts of airtightening retrofits on ventilation rates and energy consumption in a manufactured home. Energy Buildings (2011), doi:10.1016/j.enbuild.2011.07.027

Nagda, N.L., Harrje, D.T., Koontz, M.D. and Purcell, G.G. A detailed investigation of the air infiltration characteristics of two houses. Measured Air Leakage of Buildings. ASTM STP 904. Philadelphia, PA: 33-45. 1986.

Ochsendorf, J., Norford, L., Brown, D., Durschlag, H., Hsu, S., Love, A., Santero, N., Swei, O., Webb, A., Wildnauer, M. Methods, Impacts, and Opportunities in the Concrete Building Life Cycle, Massachusetts Institute of Technology Concrete Sustainability Hub. Cambridge, MA. 2011.

Persily, A.K. Myths about building envelopes. ASHRAE Journal 41:39–48. 1999.

Persily, A., Musser, A., and Leber, D. "A Collection of Homes to Represent The US Housing Stock" NISTIR 7330, NIST, 2006.

Petrie, T.W., Kosny, J., Desjarlais, A.O., Atchley, J.A., Childs, P.W., Ternes, M.P., and Christian, J.E. How ICF versus Conventional Construction of Exterior Walls Affects Whole Building Energy Consumption: Field Study and Simulation. Oak Ridge National Lab. 2002.

Purdy, Beausoleil-Morrison. The Significant Factors in Modeling Residential Buildings. Seventh International IBPSA Conference Rio de Janeiro, Brazil August 13-15. 2001.

Rajagopalan, N., Bilec, M.M., Landis, A.E. Comparative Life Cycle Assessment of Insulating Concrete Forms with Traditional Residential Wall Sections. ISSST, 1-5. 2009 IEEE International Symposium on Sustainable Systems and Technology. 2009.

Reinhold, C. and Sonderegger, R. Component Leakage Areas in Residential Buildings. Air Infiltration Reduction in Residential Buildings. 4th AIC Conference. Switzerland. September 1983.

Rice, J.A. Mathematical statistics and data analysis 3rd ed. Brooks/Cole: California, 2007.

Shaw, C.Y., Sander, D.M., and Tamura, G.T. Air Leakage Measurements of the Exterior Walls of Tall Buildings. ASHRAE Transactions. 79: 40-48. 1973.

Shaw, C.Y., and Jones, L. Air Tightness and Infiltration of School Buildings. National Research Council of Canada, reprinted from ASHRAE Transactions. 85: 85-95. 1979.

Sherman, M. H. Air Infiltration in Buildings. Lawrence Berkeley Lab. AIP Conference Proceedings 135: 655-662. 1985.

Sherman, M.H., and Chan, R. Building Airtightness: Research and Practice. Lawrence Berkeley National Laboratory, report no. 53356, 2004.

Sherman, M.H., and Grimsrud, D.T. Measurement of Infiltration Using Fan Pressurization and Weather Data. Presented at the First Symposium of the Air Infiltration Centre of Instrumentation and Measurement Techniques. Windsor, England. 1980.

Sherman, M.H., Matson, N.E. "Air Tightness of New US Houses." LBNL-48671. Berkeley, CA. 2002.

Stephens, M. A. EDF Statistics for Goodness of Fit and Some Comparisons. Journal of the American Statistical Association (American Statistical Association). 69 (347): 730–737. 1974.

Tamura, G.T. and Shaw, C.Y. Studies on Exterior Wall Airtightness and Infiltration of Tall Buildings. ASHRAE Transactions 82: 122-134. 1977.

US Census. Median and Average Square Feet of Floor Area in New Single-Family Houses Completed by Location. <http://www.census.gov/const/C25Ann/sftotalmedavgsqft.pdf> Accessed January 2012.

US Department of Energy. Air Sealing: A Guide for Contractors to Share with Homeowners. Pacific Northwest and Oak Ridge National Laboratory. 2010. <http://apps1.eere.energy.gov/buildings/publications/pdfs/building_america/ba_airsealing_report.pdf>

US Department of Energy. International Energy Conservation Code. 2009.

US Department of Energy. EnergyPlus 6.0. 2010.

US Environmental Protection Agency. Air Seal and Insulate with Energy Star. <http://www.energystar.gov/index.cfm?c=home_sealing.hm_improvement_sealing> Accessed February 2012.

VanBronkhorst, D. A.; Persily, A. K.; Emmerich, S. J. Energy Impacts of Air Leakage in U.S. Office Buildings. Implementing the Results of Ventilation Research. AIVC Conference, 16th. Proceedings: 379-391. Palm Springs, CA. 1995.

Walpole, R.E., Myers, R. H., Myers, S.L., Ye, K. Probability and Statistics for Engineers and Scientists. Ed 8. Pearson Prentice. 2007.

Appendix A: Code Used for Analysis in Section 3.2

This appendix lists all of the code used in the analysis of the data. The data was entered manually into the code. However, due to its length, the numbers are removed and replaced with [. . .].

```
data = [...]

test = [...]
valid = [...]
valid_noNaN = [...]
valid_nooutlier = [...]
test_noNaN = [...]

%plot all of the data
data_all = [...];
figure1 = figure('Color',[1 1 1]);
[N,xout] = hist(data_all,10);
xout=round(xout);

hist(data_all,10)
h = findobj(gca,'Type','patch');
set(h,'FaceColor','k')
set(gca,'XTick',xout,'fontsize',10)
xlabel('Air Leakage, cm2','Fontsize',20)
ylabel('Number of Houses','Fontsize',20)

%plot the 31 points
figure2 = figure('Color',[1 1 1]);
[N,xout] =hist(data(:,1),10);
xout=round(xout);

hist(data(:,1),10)
h = findobj(gca,'Type','patch');
set(h,'FaceColor','k')
set(gca,'XTick',xout,'fontsize',10)
xlabel('Air Leakage, cm2','Fontsize',20)
ylabel('Number of Houses','Fontsize',20)
```

Appendix B: Chart Used to Collect Blower Door Data

GENERAL TEST INFORMATION

Date of Air Tightness Test	
Rater Data	
Name	
Company Name	
Address	
Email	
Are you certified by RESNET? (Y-yes, N-no)	
Are you certified by other home raters association? Please give the name of the	
Name and Number of the code you used for the Air Infiltration Test (ASTM E 779-03 for Fan Pressurization or ASTM E 1827-96 for Orifice Blower Door Test)	

ICF HOUSE GENERAL INFORMATION

Climate Zone (according to ASHRAE)	
Locale	
City	
Street	
Zipcode and State	
County	
Year of construction	
Envelope construction type	
Number of stories	
Total floor area of the building [ft2] including unconditioned spaces	
Total floor area of conditioned space [ft2]	
Perimeter	
Number of occupants	

HOUSE GENERAL GEOMETRY INFORMATION

Estimated House Volume	
Does the house have a basement? (Y-yes, N-no)	
basement floor area	
basement height	
is basement conditioned? (Y-yes, N-no)	
1st story	
1st story floor area [ft2]	
1st story height [ft]	
is 1st story conditioned? (Y-yes, N-no)	
2nd story*	
2nd story floor area	
2nd story height	
is 2st story conditioned? (Y-yes, N-no)	
Attic*	
Attic floor area [ft2]	
Attic height [ft]	
is Attic conditioned? (Y-yes, N-no)	
Roof type (pitched or flat)	
or (if above mentioned data is impossible to collect)	
Total house volume	
Conditioned area volume	
Unconditioned area volume (basement, attic, vestibules)	

OTHER INFORMATION

Foundation type	

ENVELOPE DATA

1st Floor					**2nd Floor - NA**			
	width	height	type of opening			width	height	type of opening
Wall 1					**Wall 1**			
Main Door					Main Door			
Window 1					Window 1			
Window 2					Window 2			
Wall 2					**Wall 2**			
Window 1					Window 1			
Window 2					Window 2			
Wall 3					**Wall 3**			
Window 1								
Window 2								
Wall 4					**Wall 4**			
Window 1								
Window 2								
Wall 5					**Wall 5**			
Window 1								
Window 2								
Wall 6					**Wall 6**			
Window 1								
Window 2								
Wall 7					**Wall 7**			
Window 1								
Window 2								
Wall 8					**Wall 8**			
Window 1								
Window 2								
Wall 9					**Wall 9**			
Window 1								
Window 2								
Wall 10					**Wall 10**			
Window 1								
Window 2								
Number of windows								
Area of windows (sf)								
Number of doors								
Area of doors (sf)								

HVAC

HVAC system (Heating & cooling, what type & what fuel)	
Heating System	
Heating Fuel	
Cooling System	
Cooling Fuel	
With or without mechanical ventilation	

OTHERS OPENINGS

Fireplaces	
Number of fireplaces in the 1st floor	
Number of fireplaces in the 2nd floor	
Number of Bathrooms	
Number of exhaust fans in Bathroom 1	
Number of exhaust fans in Bathroom 2	
Number of exhaust fans in Bathroom 3	
Number of exhaust fans in Bathroom 4	
Number of Kitchens	
Number of exhaust fans in Kitchen 1	
Number of exhaust fans in Kitchen 2	
Others visible openings	

TEST DATA

Wind speed	
Building floor plan with located Envelope Pressure Sensors (sketch)	
Temperature inside at the beginning [F]	
Temperature outside the building at the beginning [F]	
Temperature inside building at the end of the test (if changed) [F]	
Temperature outside building at the end of the test (if changed) [F]	

* Pressures and fan speeds averaged over at least 10-s time period, for at least 10 data points. Pressure should range from 10 to 60 Pa.

Supply ducts cloed		**Supply ducts opened**	
Nominal Building Presuure [Pa]	Nominal Flow [cfm]	Nominal Building Presuure [Pa]	Nominal Flow [cfm]

TEST RESULTS

device specification (type, rande, date of last calibration)		
Leakage Area	supply ducts closed	supply ducts opened
Calculated Leakage Area Canadian EqLA @ 10Pa [in2]		
Calculated Leakage Area LBL ELA @ 4 Pa [in2]		
Airflow at 50Pa	supply ducts closed	supply ducts opened
CFM at 50 Pa [cfm]		
Calculated Air Change per Hour (ACH) at 50Pa		
Estimated Average Infiltration rate	supply ducts closed	supply ducts opened
Estimated Average Annual ACH		
Estimated Average Annual CFM		

ATTACHMENTS REQUIRED

A.1. Air tightness protocol
A.2. Pictures/Photos of envelope from each side of building, with indication of orientation and story (eg. 2nd story windows on wall facing South)
A.3. Close-up pictures/photos of each openings (windows/doors/vents)

Appendix C: Leakage Area, Floor Area and Height of the 31 Houses in the Dataset

	Leakage Area (cm2)	Floor Area (ft2)	Height (ft)
16410 N Shore Ct.	522.34	4076	19.0
1226 A Russell Drive	251.71	840	8.3
7392 Wellington Rd 11	401.14	5103	20.8
1087 Henry Street	163.13	3326	9.8
40 Cody Dr	208.37	3360	9.8
3026 SW Ellsworth Ave	118.59	2587	19.0
818 Westford Rd	585.63	3411	8.0
225 NW Bayshore Blvd	414.88	2721	19.0
158 Webster Rd.	454.73	4458	9.0
7506 Nolensville RD	983.61	4440	20.0
6520 East Bay Blvd	720.31	3079	18.0
1461 Hwy 98 West	325.61	3440	17.0
5720 Pinewood RD	1389.00	6311	11.2
6020 Woodland Hills Drive	1188.46	5101	18.0
4341 Arno Road	2608.11	5040	22.0
1953 Edenbridge Way	785.44	3341	18.0
1205 Haber Drive	1264.87	4462	17.5
1064 Bills Lane	494.33	2405	9.0
108 Fern Avenue	1351.81	3912	19.3
6919 Comstock Road	1632.60	3392	18.0
6027 Woodland Hills Drive	1163.39	5715	18.0
1522 Bear Branch Cove	1309.19	6085	20.0
3365 Timber Trace	865.98	4196	9.0
9014 Groveland	648.29	2431	10.0
9010 Groveland	906.20	3259	18.0
8930 Groveland	719.59	3199	18.0
9011 Groveland	287.89	2796	26.0
8803 San Leandro	834.56	2397	18.0
8723 Santa Clara Drive	309.15	2656	9.0
6300 Elm Crest Ct	999.52	5482	20.0
162 Sandstone Lane	684.43	2697	10.0

Appendix D: ASTM Uncertainty Calculation

1. Calculate the variance of n

$$S_n^2 = \frac{1}{S_{\ln(dP)}}\left(\frac{S_{\ln(Q)}^2 - n * S_{\ln(dP)\ln(Q)}}{N-2}\right)^{1/2}$$

2. Calculate the variance of ln(C)

$$S_{\ln(C)}^2 = S_n\left(\frac{\sum_{i=1}^{N} dP_i^2}{N}\right)^{1/2}$$

3. Calculate the 95% confidence interval for ln(C) using a T distribution

$$I_{\ln(C)} = S_{\ln(C)}^2 * T(95\%, N-2)$$

4. Calculate the upper and lower limits of leakage area at the reference pressure $dP_r = 4$

$$A_L upper = A_L \exp(I_{\ln(C)} \ln(dP_r))$$
$$A_L lower = A_L \exp(-I_{\ln(C)} \ln(dP_r))$$

5. The uncertainty is then given as

$$uncertaint\,y = \frac{A_L upper - A_L lower}{2}$$

Appendix E: Code Used for Analysis in Section 3.3

```
%Determine the distribution
%test to see if the data or the log(data) is normally distributed
B = kstest(data(:,1))
C = kstest(log_data)

%fit a gamma distibution using method of maximum likelihood
figure = figure('Color',[1 1 1]);
hist(data(:,1),10)
[n, xout] = hist(data(:,1),10)
histarea = sum(range(data(:,1))/10*n);
[MLEgamma,intevalgamma] = gamfit(data(:,1))
x=[0:10:3000];
ygamma = histarea*gampdf(x,MLEgamma(1),MLEgamma(2));
hold on
plot(x,ygamma,'color','r')
title(' ','FontSize',18)
legend('data','gamma')
xlabel('Air Leakage, cm2','Fontsize',20)
ylabel('Number of Houses','Fontsize',20)
set(gca, 'fontsize',18)
h = findobj(gca,'Type','patch');
set(h,'FaceColor','k')
xout=round(xout)
set(gca,'XTick',xout,'fontsize',10)

%test to see if gamma distribution is the same as the data
D = kstest(data(:,1),[x' gamcdf(x, MLEgamma(1),MLEgamma(2))'])

%bootstrap the data itself and take the mean of each sample
for i = 1:1000
b = randsample(data(:,1),10);
meanb = mean(b);
X(i) = meanb;
end
figure = figure('Color',[1 1 1]);
hist(X)
ylabel('Number of Houses','Fontsize',15)
xlabel('Leakage area, cm2','Fontsize',15)
h = findobj(gca,'Type','patch');
set(h,'FaceColor','k')
[N,xout] = hist(X)
xout=round(xout)
set(gca,'XTick',xout,'fontsize',10)

%mean of all the data
m = mean(data(:,1))

%variability based on ASTM standard deviation
var = [...];
figure = figure('Color',[1 1 1]);

hist(var,10)
xlabel('Air Leakage, cm2','Fontsize',20)
```

```
ylabel('Number of Houses','Fontsize',20)

h = findobj(gca,'Type','patch');
set(h,'FaceColor','k')
[N,xout] = hist(var)
xout=round(xout)
set(gca,'XTick',xout,'fontsize',10)
```

Appendix F: Details of leakage prediction and code used for this analysis

The three methods used to predict air leakage are:

1. Selection of terms based on visual inspection
2. Stepwise regression
3. Regression trees

<u>Conjecture based on visual inspection</u>

A plot of the correlations of all of the variables can be seen in **Figure F.1.** The first variable is leakage area, and the others follow in the order listed in **Table 3-1.**

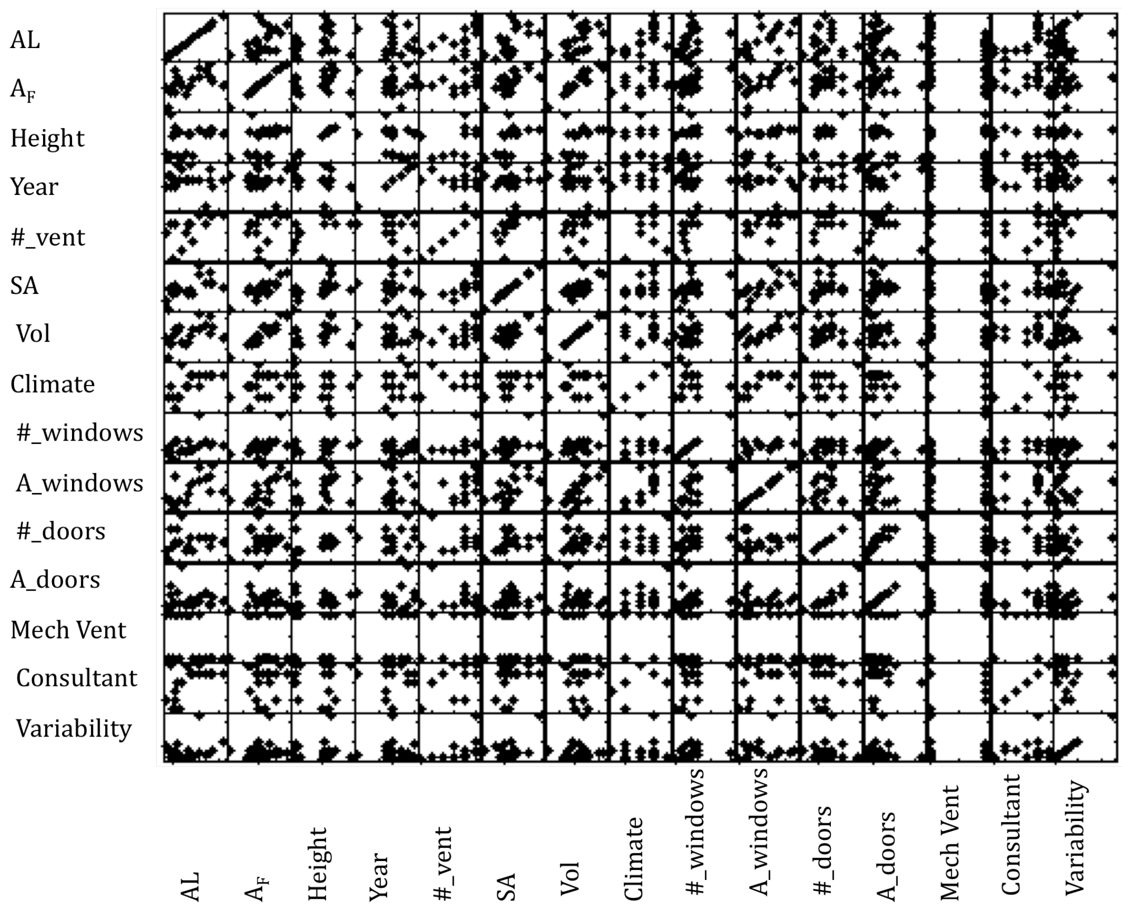

Figure F.1. Variable correlation plot to understand which aspects of the houses best correlate to leakage area and each other

Based on this chart, surface area, volume and the area of windows seem to correlate the best with air leakage. It is also clear that area of windows, number of windows, area of doors and number of doors are related. The reason for this is clear: a great number of windows and doors, especially because these elements typically come in standard sizes, can cause a larger surface area of windows and doors.

Climate and consultant also seem to be correlated. This is expected because different contractors were contacted to perform these tests in different regions of the country. Interestingly, climate also appears to be related to windows. Although it is generally believed that home design does not vary by climate, it is clear that some decisions are made, whether conscious or not, to better suit a region.
Based on this discussion, the following equations are tested:

$$B0 + B1 * volume + B2 * window\_area = leakage\_area \quad \text{(F-1)}$$

$$B0 + B1 * surface\_area + B2 * window\_area = leakage\_area \quad \text{(F-2)}$$

The residuals, the difference between the values that Equation F-1 predicts and the actual values, are relatively well spaced and therefore do not indicate that the equation must be changed. However, they have a very large range compared to the size of the data. The leakage areas range from 118 to 1632 cm^2 and the residuals between ±600 cm^2. This points to the conclusion that this equation is not the best option. The root-mean squared prediction error is 354.4 cm^2.

For Equation F-2 the residuals do not show any specific trend. Although smaller, the RMSPE, 340.2 cm^2, is still large.

Before this analysis was done, 10 data points were set aside, randomly, to use on the possible equations as validation. When Equations 3-4 and 3-5 are tested on the validation data, the root mean squared prediction errors are 555.5 and 1100 cm^2, respectively. Both RMSPE's are very large. However, after examining the validation test data, it is confirmed that the outlier seen in Figure 3.2 is in this set. Therefore, a method that does not place as much emphasis on outliers is required. Using medians as opposed to means is a good way to avoid skewing the results. Therefore, the median absolute errors are computed using the following formula:

$$Median\ Absolute\ Error = Median(abs(errors - median(errors))) \quad \text{(F-3)}$$

The values calculated are 164.2 and 234.0 cm^2, which are much more reasonable numbers. In this case, Equation F-1 has less error.

Finally, the outlier is removed from the validation data and the RMSPE is re-calculated. This method simply calculates the error, ignoring the presence of an outlier. For Equation F-1 the new RMSPE error is now 151.1 cm^2, and 128.9 cm^2 for Equation F-2. Equation F-2 is found to create less error, as opposed to the results found when median error is calculated. Because of this discrepancy, other tests, including stepwise regression and regression trees, are performed, as discussed below.

Stepwise regression

Because the errors generated above based on visual conjecture are not consistent, another method of determining the most important variables is necessary. Stepwise regression uses a repeating procedure, testing each variable to see if it is valuable enough for predictive purposes. The program will then print which variables are important for predicting air leakage. When this method is implemented, volume is the only variable chosen. Based on this result, Equation F-4 is found using linear regression:

$$Air\ leakage = -12.56 + .0006 * volume \qquad (\text{F-4})$$

where
Volume = m^3
Air leakage = cm^2

Although not guessed in the previous section, this is similar to **Equation F-1**, above. The RMSPE of the entire model is 345.7 cm^2, which is similar to the error in **Equations F-1** and **F-2**, above.

On the validation data, the median absolute error is 225.6 cm^2. Again, this is slightly greater than the error found when using volume and area of windows. The RMSPE with the outlier removed is 200, which is greater than the equivalent error for the equations above.

Although it appears that volume and area of windows are the most important variables for prediction, another statistical tool is well suited for this process: regression trees. These are implemented to explore another technique, and the results are discussed in the next section.

Regression Trees

Regression trees approach the data by "splitting" it based on the most predictive variable. This split creates two subsets of data, which are then split again based on the best predictive variable in that instance. This cycle continues until there are no more splits that increase the accuracy of the prediction.

When all of the variables listed in section 3.4.3 are considered, the tree created can be seen in Figure F.2.

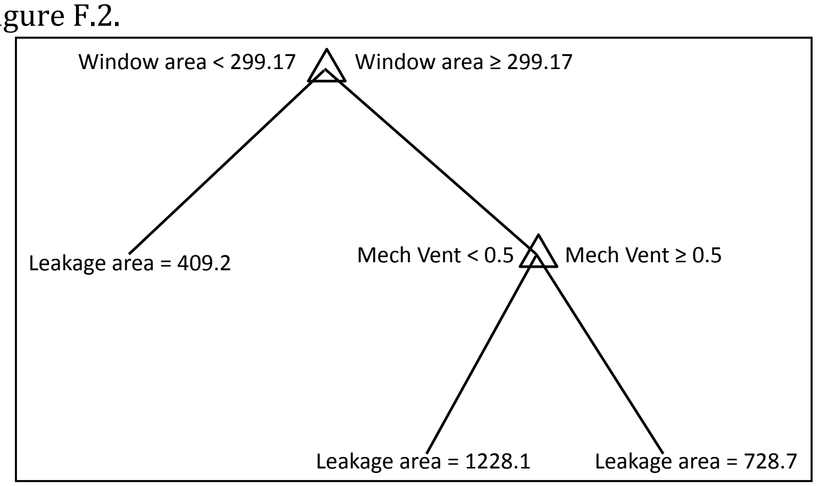

Figure F.2. The regression tree displays that window area and the presence of mechanical ventilation are important for predicting leakage area.

The error for this method is in **Table F-1**. It includes the RMSPE of the test data, the RMSPE of the validation data, with and without the outlier, and the median absolute error of the validation data.

Table F-1. The different types of error that the regression tree produces are similar to the error of other equations.

		Without outlier
RMSPE	215.4	
RMSPE_valid	517.2	223.3
Median Error_valid	187.9	

These errors are similar to those obtained based on visual conjecture and stepwise regression. Interestingly, the RMSPE is smaller while the median error is larger.

<u>Code used to do this analysis</u>

```
data = [...];
%randomly select 21 test data points and 10 validation points
r = randperm(31);
test = data(r(1:21)',:);
valid = data(r(22:31)',:);
ylabel('Number of Houses','Fontsize',20)


figure = figure('Color',[1 1 1]);
gplotmatrix(test,test,[],'k','.',6)

set(gca,'Xticklabel',[]);

%AL, Floor area, Height, Year, # of vents, SA, Vol, Climate, # Windows,
Area windows, # doors, Area doors, Mech Vent, Consultant, variability

%B0 + B1*volume + B2*area of windows
    fprintf('B0 + B1*volume + B2*area of windows \n')

    B = regstats(test(:,1),[test(:,7) test(:,10)]);
    figure = figure('Color',[1 1 1]);
    subplot 121; plot(test(:,7),B.r,'.')
    ylabel('Residuals, cm2 ','Fontsize',20)
    xlabel('Volume, ft3','Fontsize',20)
    fprintf('B0   =   %g,   B1   =   %g,   B2   =   %g   \n',B.beta(1),
B.beta(2),B.beta(3))
    subplot 122; plot(test(:,10),B.r,'.')
    xlabel('Area of windows, ft2','Fontsize',20)

    fprintf('The root mean squared error is %g',sqrt(B.mse))

    %test validation data
    fit          =          B.beta(1)*ones(size(valid_noNaN(:,1)))          +
B.beta(2)*valid_noNaN(:,7) + B.beta(3)*valid_noNaN(:,10);
    RMSE = sqrt(sum((fit-valid_noNaN(:,1)).^2)/10)
    medianerror1   =   median(abs((fit-valid_noNaN(:,1))   -   median(fit-
valid_noNaN(:,1))))
```

```
    fit = B.beta(1)*ones(size(valid_nooutlier(:,1))) + B.beta(2)*valid_nooutlier(:,7) + B.beta(3)*valid_nooutlier(:,10);
    RMSE2 = sqrt(sum((fit-valid_nooutlier(:,1)).^2)/10)

%B0 + B1*surface area + B2*area of windows
    fprintf('B0 + B1*surface area + B2*area of windows \n')
    figure1 = figure('Color',[1 1 1]);
    B = regstats(test(:,1),[test(:,6) test(:,10)]);
    subplot 121; plot(test(:,6),B.r,'.')
    ylabel('Residuals, cm2 ','Fontsize',20)
    xlabel('Volume, ft3','Fontsize',20)
    fprintf('B0 = %g, B1 = %g, B2 = %g \n',B.beta(1), B.beta(2),B.beta(3))
    subplot 122; plot(test(:,10),B.r,'.')
    xlabel('Area of windows, ft2','Fontsize',20)

    fprintf('The root mean squared error is %g',sqrt(B.mse))

    %test validation data
    fit = B.beta(1)*ones(size(valid_noNaN(:,1))) + B.beta(2)*valid_noNaN(:,6) + B.beta(3)*valid_noNaN(:,10);
    RMSE = sqrt(sum((fit-valid_noNaN(:,1)).^2)/10)
    medianerror2 = median(abs((fit-valid_noNaN(:,1)) - median(fit-valid_noNaN(:,1))))
    fit = B.beta(1)*ones(size(valid_nooutlier(:,1))) + B.beta(2)*valid_nooutlier(:,6) + B.beta(3)*valid_nooutlier(:,10);
    RMSE2 = sqrt(sum((fit-valid_nooutlier(:,1)).^2)/10)

%Stepwise Regression
[b,se,pval,inmodel,stats,nextstep,history] = stepwisefit(test(:,2:14),test(:,1));
fit = -12.56 + .0213*test_noNaN(:,7);
RMSE = sqrt(sum((fit-test_noNaN(:,1)).^2)/15)

fit = -12.56*ones(size(valid_noNaN(:,1))) +.0213*valid_noNaN(:,7);
medianerror = median(abs((fit-valid_noNaN(:,1)) - median(fit-valid_noNaN(:,1))))
ValidRMSPE = sqrt(sum((fit-valid_noNaN(:,1)).^2)/10)

fit = -12.56*ones(size(valid_nooutlier(:,1))) +.0213*valid_nooutlier(:,7);
RMSE2 = sqrt(sum((fit-valid_nooutlier(:,1)).^2)/10)

%Regression Trees
T = classregtree(test(:,2:15),test(:,1),'method','regression','names',{'Floor Area' 'Height' 'Year' 'Number of Vents' 'Surface Area' 'Volume' 'Climate' '#Windows' 'Window Area' '#doors' 'Door Area' 'Mech Vent' 'Consultant' 'Variability'});
view(T);

Ynew = eval(T,test(:,2:15));
RMSPE = sqrt(sum((Ynew-test(:,1)).^2)/21)

Yvalid = eval(T,valid(:,2:15));
ValidRMSPE = sqrt(sum((Yvalid-valid(:,1)).^2)/10)
```

```
medianerror    =    median(abs((Yvalid-valid(:,1))    -    median(Yvalid-
valid(:,1))))

Yvalid = eval(T,valid_nooutlier(:,2:15));
ValidRMSPE = sqrt(sum((Yvalid-valid_nooutlier(:,1)).^2)/7)
```

Appendix G: Code Used for Analysis in Section 3.5

```
%Plot NL
NL = 0.1.*(data(:,1)./data(:,2)./0.0929).*((data(:,3).*.3048/2.5).^.3)

box_NL = boxplot(NL);
get(GCF);
get(gca);
set(GCF, 'Color',[1 1 1]);
set(gca,'XTickLabel',{''});
ylabel('Normalized Leakage','Fontsize',20)
ylim([0 .85]);
set(gca, 'fontsize',18)

line([0 ; 2],[.57 ; .57],'color','k');
annotation('textbox',[.13 .69 1 .01], 'String','ASHRAE 119 (Chicago
maximum)','linestyle','none');

line([0 ; 2],[.24 ; .24],'color','k');
annotation('textbox',[.13 .36 1 .01], 'String','[Persily, 2006] Floor
area > 148.6 m2','linestyle','none');
line([0 ; 2],[.31 ; .31],'color','k');
annotation('textbox',[.13 .46 1 .01], 'String','[Persily, 2006] Floor
area < 148.6 m2','linestyle','none');

line([0 ; 2],[.55 ; .55],'color','k');
annotation('textbox',[.13 .65 1 .01], 'String','[Sherman, 2002] Avg for
new, conv. homes','linestyle','none');
```